

Thesis Number: MEE05:34



Peak to Average Ratio Reduction in Wireless OFDM Communication Systems

Kamran Haider

**This thesis is presented as part of the Degree of Master of Science in
Electrical Engineering
Blekinge Institute of Technology**

January 2006

Master of Science in Electrical Engineering
Blekinge Institute of Technology
Department of Telecommunications and signal processing
Examiner: Dr. Abbas Mohammed
Supervisors: Dr. Abbas Mohammed, Blekinge Institute of technology
Robert Baldemair, Access technologies Ericsson Research, Ericsson AB

Abstract

Future mobile communications systems reaching for ever increasing data rates require higher bandwidths than those typical used in today's cellular systems. By going to higher bandwidth the (for low bandwidth) flat fading radio channel becomes frequency selective and time dispersive.

Due to its inherent robustness against time dispersion Orthogonal Frequency Division Multiplex (OFDM) is an attractive candidate for such future mobile communication systems.

OFDM partitions the available bandwidth into many subchannels with much lower bandwidth. Such a narrowband subchannel experiences now due to its low bandwidth an almost flat fading leading in addition to above mentioned robustness also to simple implementations. However, one potential drawback with OFDM modulation is the high Peak to Average Ratio (PAR) of the transmitted signal: The signal transmitted by the OFDM system is the superposition of all signals transmitted in the narrowband subchannels. The transmit signal has then due to the central limit theorem a Gaussian distribution leading to high peak values compared to the average power.

A system design not taking this into account will have a high clip rate: Each signal sample that is beyond the saturation limit of the power amplifier suffers either clipping to this limit value or other non-linear distortion, both creating additional bit errors in the receiver.

One possibility to avoid clipping is to design the system for very high signal peaks. However, this approach leads to very high power consumption (since the power amplifier must have high supply rails) and also complex power amplifiers.

The preferred solution is therefore to apply digital signal processing that reduces such high peak values in the transmitted signal thus avoiding clipping. These methods are commonly referred to as PAR reduction. PAR reduction methods can be categorized into transparent methods – here the receiver is not aware of the reduction scheme applied by the transmitter – and non-transparent methods where the receiver needs to know the PAR algorithm applied by the transmitter. This master thesis would focus on transparent PAR reduction algorithms. The performance of PAR reduction method will be analysed both with and without the PSD constrained. The effect of error power on data tones due to clipping will be investigated in this report.

Acknowledgement

I am grateful to my supervisor Robert Baldemair at Ericsson AB Kista, Stockholm for his help, constant consultation and guidance during my thesis work. I would also like to thank Mikael Höök for his time to review my report.

I would also like to express gratitude to Dr. Abbas Mohammed who is my supervisor and examiner at Blekinge Institute of Technology. Many thanks to him for supporting and encouraging me.

Finally this work could not have been performed with the support of my parents, my brother and my wife who have always loved and encouraged me

Contents

1	Introduction.....	5
2	Background	6
2.1	THE OFDM SYSTEM	7
2.2	OFDM SIGNALS.....	8
2.3	PEAK TO AVERAGE RATIO	9
2.4	PAR REDUCTION METHODS	11
2.4.1	<i>Transparent Methods</i>	11
2.4.2	<i>Non Transparent Methods</i>	12
3	Tone Reservation	14
3.1	Problem Formulation	15
3.1.1	<i>PAR Reduction Signal for Tone Reservation</i>	17
3.1.2	<i>Optimal Tone Reservation: Real-Baseband Case</i>	19
3.1.3	<i>Optimal Tone Reservation: Complex-Baseband Case</i>	23
4	Tone Reservation Kernel Design.....	25
5	Active-Set Methods	27
6	Practical Active-Set Tone Reservation	28
6.1	DETERMINING DESCENT DIRECTION.....	28
6.2	DETERMINING THE SIGNAL NEXT ACTIVE CONSTRAINT	29
6.3	COMPLETE ACTIVE-SET ALGORITHM	31
6.4	EXTENSION TO THE COMPLEX-BASEBAND CASE.....	31
7	PSD constrained Tone reservation.....	33
8	PSD-constrained active-set approach.....	36
9	Simulation and Results.....	38
9.1	PAR REDUCTION GAIN WITH ACTIVE-SET ALGORITHM	40
9.3	INVESTIGATION OF NUMBER OF ITERATIONS REQUIRED TO ACHIEVE A DESIRED PAR REDUCTION	46
9.4	INVESTIGATION OF ERROR POWER ON THE DATA TONES AFTER ACTIVE-SET METHOD	49
9.5	ANALYSIS OF PSD CONSTRAINTS ON THE RESERVED TONES	51
9.6	EFFECT OF NUMBER OF RESERVED TONES.....	54
10	Conclusions.....	56
11	Future work	57
12	References	58

1 Introduction

In the recent years a lot of advancements have been done in the multimedia technology and services. To enable these services with mobile communication high data rates and efficient usage of the available spectrum is required. Much research is on going to investigate transmission methods that can provide high data rates, can cope with multipath propagation, provide robustness against frequency selective fading or narrowband interference, and require less power and cost.

Multicarrier modulation is one technique that provides us the desired demands of high data rates. Orthogonal Frequency Division Multiplexing (OFDM) is a form of multicarrier modulation that can be seen either as modulation technique or a multiplexing scheme. OFDM is considered as a very promising candidate for future mobile communication systems. OFDM uses the Inverse Fast Fourier Transform (IFFT) operation to generate a large number of subchannels that are orthogonal. A cyclic prefix is added in the time domain that simplifies equalization and also eliminates *interblock interference* (IBI). OFDM is a widely used communication technique in broadband access applications requiring high data rates. It is already used in different WLAN standards (HIPERLAN 2, IEEE 802.11a), ADSL and digital video broadcasting (DVB). Even though OFDM has a number of advantages it has a potential drawback of high Peak to Average Power Ratio (PAPR). This high peak to average ratio causes nonlinearities in the transmitted signal and also degrades the power efficiency of the system. In order to reduce the PAR problem many researcher have made efforts and a large variety of different PAR reduction approaches are proposed. In this thesis work we also focus on the problem of high PAR and a novel approach for PAR reduction along with a practical algorithm will be discussed. In practical systems the data carrying subchannels are under the restriction of limited power. The analysis of a PSD constrained on the reserved tones and on the data tones, the number of reserved tones, and the effect of reserved tones on the data tones is also a part of this thesis work.

2 Background

In the recent year's multicarrier modulation has become a key technology for current and future communication systems and *Orthogonal Frequency Division Multiplexing* (OFDM) is a form of multicarrier modulation. These systems are becoming popular due to the fact that they efficiently use the available frequency band and provide high data rates. In the multicarrier modulation the available frequency band is divided into a large number of subbands and the user data is modulated onto many separate subcarriers. These subcarriers are separated from each other and in case of OFDM the subcarrier are orthogonal to each other. To achieve orthogonality between the different subcarriers the spacing between the carriers is equal to the reciprocal of the useful symbol period. The spectrum of these subcarriers shows that each subcarrier has a null at the centre frequency of the other subcarriers in the system, which is shown in the Figure 1.1. When the subcarriers are placed in this fashion then there is no interference between the different carriers.

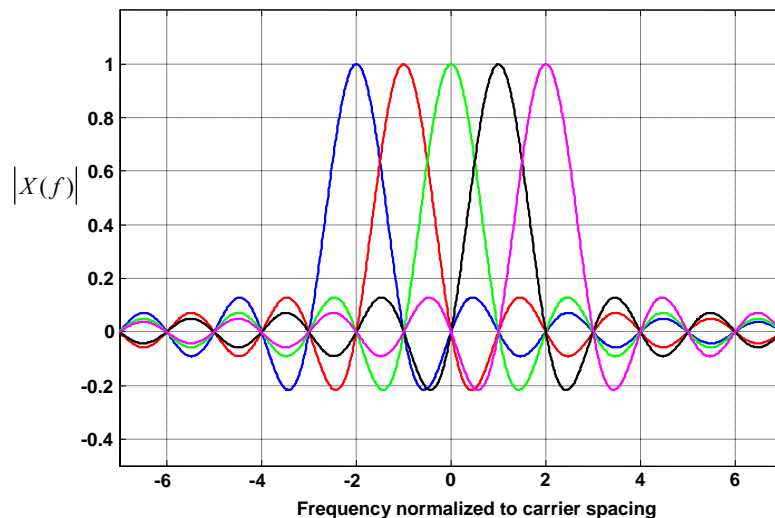


Figure 1.1: Frequency-domain representation of a multicarrier signal

If we compare a multicarrier modulation system (OFDM in our case) with a single carrier modulation system then the multicarrier system has several advantages: Multicarrier systems offer a better immunity for multipath effects, channel equalization is much simpler and timing acquisition constraints are relaxed. Some advantages and disadvantages of OFDM compared to single carrier modulation are summarized below:

Advantages:

1. Interblock interference (IBI) is almost eliminated in OFDM because a cyclic prefix is added to the time domain signal.
2. OFDM is more resistive to frequency selective fading than single carrier systems because it divides the channel into narrowband flat fading subchannels.

3. A cyclic prefix is added at the transmitter side in the OFDM, which makes the channel equalization simpler than in single carrier systems where adaptive equalization techniques are used.
4. As compare to single carrier systems, OFDM systems offer a better immunity against sample timing offsets, co- channel interference, and impulsive parasitic noise.
5. Maximum likelihood decoding becomes more feasible in OFDM system especially together with MIMO.
6. FFT techniques to implement the modulation and demodulation functions increase the computational efficiency of OFDM system.

Disadvantages:

1. The OFDM signal suffers from a high peak to average ratio.
2. In OFDM the effects of local frequency offset and radio front-end non-linearities are more severe than in single carrier systems.
3. The addition of cyclic prefix causes overhead in the OFDM system.

2.1 The OFDM System

A typical OFDM transmission system is shown in Figure 2.2. Here an input data bit stream is supplied into a channel encoder that separates the data into N different subchannels. Then that data are mapped onto QPSK/QAM constellation. After this mapping of the data an N -point IFFT is applied to transform the frequency domain incoming symbols into the time domain signal. This transformation maps the data points onto orthogonal subcarriers. A cyclic prefix is added to the signal in the digital domain after the IFFT operation to avoid *interblock interference* (IBI). The cyclic prefix is a copy of the last samples in time domain that are inserted at the beginning of the block. This time domain signal then under- goes a parallel to serial conversion and an analog signal is generated by using a D/A converter. Finally filtering with a low-pass filter is applied, and this filtered signal is modulated to the desired carrier frequency, which is then sent across the channel for transmission.

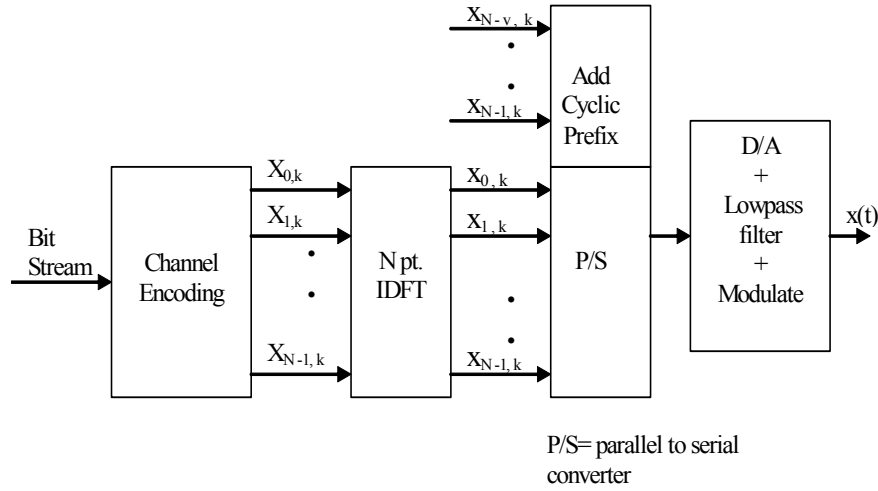


Figure 2.2: Block diagram of an OFDM transmitter.

To recover the information in the OFDM receiver the inverse operations to the operations listed above are performed in the reverse direction. In the receiver we start with the demodulated of the signal to get the baseband signal. Then this baseband signal is filtered. Now the signal undergoes analog to digital conversion in an A/D converter. The cyclic prefix which was added at the transmitter side is removed and an N point FFT operation is performed on the resulting signal to recover the data in frequency domain. A frequency domain equalizer consisting of N single tap complex equalizers is applied to the frequency domain data and its output is fed into a channel decoder, which finally decodes the transmitted bit stream.

2.2 OFDM Signals

In the previous section a typical OFDM system is described briefly, in this section we will mathematically describe the different signals at the various stages of above system. We suppose that we use Quadrature Amplitude Modulation (QAM) so when the input bit stream is fed to the channel encoder then this bit stream will be mapped into QAM symbols to create the m -th complex-valued OFDM symbol vector $\mathbf{X}^m = [X_0^m \dots X_{N-1}^m]^T$. This complex-valued OFDM symbol vector is now applied to an N point IDFT operation to form a discrete time signal i.e.

$$\mathbf{x}^m = \mathbf{x}^m[n] = \frac{1}{\sqrt{N}} \sum_{k=0}^{N-1} X_k^m \exp^{j2\pi kn/N}, \quad k = 0, 1, \dots, N-1 \quad (2.1)$$

This discrete time signal block of parallel data is converted to a serial data stream and a cyclic prefix (CP) is added. To apply the cyclic prefix we copy the last samples of $\mathbf{x}^m[n]$ and insert them in the beginning of $\mathbf{x}^m[n]$. The new discrete time signal including cyclic prefix can be written mathematically as:

$$\mathbf{x}_k^m[n] = \frac{1}{\sqrt{N}} \sum_{k=0}^{N-1} X_k^m \exp^{j2\pi kn/N} \quad n = -\nu, -\nu + 1, \dots, 1, N-1 \quad (2.2)$$

where ν is the length of cyclic prefix. This discrete time cyclic prefixed signal is oversampled by a factor of L to form the signal $x^m[n/L]$. After the signal is oversampled, digital filtering and/or windowing is applied. Any one or both of above operations help us to satisfy any power spectral density (PSD) constraint on the resulting OFDM signal. Another point that must be noted here is that in this thesis we are applying a rectangular window, so we may expect a large PSD outside of the nominal bandwidth.

2.3 Peak to Average Ratio

In this section we will look at the cause of the high peak to average ratio problem of OFDM systems and will also see some of the drawbacks of it. If we start from the beginning with the generation of the OFDM signal we can say that the input data stream which is encoded into QAM constellations forms a symbol vector \mathbf{X}^m whose elements are independent random variables. When we take an N point IFFT we simply transform these data points from one domain into another domain by a linear combination. Now the central limit theorem of probability theory states that a linear combination of a large number of independent random signals is approximated by Gaussian. In a typical OFDM system the value of N is large so the OFDM symbol can be approximated by a Gaussian distributed signal. This implies that some samples have a high probability of large peaks. The drawbacks and problems of high PAR are explained in detail in [2] and we will here present some of them.

To transmit a signal that has high peaks requires from the power amplifier in the transmitter to have a high signal span. Such amplifiers consume high power and are also costly. If we lower the average power of the signal then this will also lower the peaks that a power amplifier needs to handle. However reducing the average power of the signal will reduce the SNR at the receiver thus degrading performance.

If we do not lower the average power of the amplifier input signal but we do not allow large peaks to pass through the amplifiers means we clip high signal peaks. This clipping introduces nonlinearities into the transmitted OFDM symbol. These nonlinearities cause an increase in bit error rate probabilities and also lead to higher out of band spectrum due to higher order harmonics.

2.4 Mathematical definition of PAR

As we have seen in the last section the basic cause of a high PAR in the OFDM signal is the Gaussian signal distribution which arises due to the large number of subchannels and their linear combination due to the IFFT operation. Now we will look at the mathematical definition of PAR. Mathematically, the PAR for a given OFDM block can be written as

$$PAR(x[n]) = \frac{\max_{0 \leq n \leq N-1} |x[n]|^2}{E\{x^2[n]\}}, \quad (2.3)$$

where $\max_{0 \leq n \leq N-1} |x[n]|^2$ denotes the maximum instantaneous power and $E\{x^2[n]\}$ denotes the average power of the signal. The peak level before and after the addition of the cyclic prefix will be same because the cyclic prefix is just a copy of a part of the original signal block. The peak power of the symbol will be the same and the average power of the symbol will not change either.

This Par definition is also denoted as block or symbol PAR. In opposite to that we can also define the sample PAR as

$$PAR(x[n_k]) = \frac{|x[n_k]|^2}{E\{x^2[n]\}}, \quad (2.4)$$

where $|x[n_k]|^2$ represents the instantaneous power of the sample k and $E\{x^2[n]\}$ denotes average power of the OFDM block.

In a practical system oversampled signals are considered and the PAR of $x[n/L]$ can be easily computed. The peak power is defined as

$$\begin{aligned} \max_n \left| x^m[n/L] \right|^2 &= \frac{1}{N} \left| \sum_{k=0}^{N-1} X_k^m \exp^{j2\pi kn/NL} \right|^2 \\ &\leq \frac{1}{N} \left[\sum_{k=0}^{N-1} \max |X_k^m| \right]^2 \end{aligned} \quad (2.5)$$

If we use the Parseval's relationship the average power can be computed as

$$E\left\{ \left| x^m[n/L] \right|^2 \right\} = \frac{1}{N} \sum_{k=0}^{N-1} E\left\{ \left| X_k^m \right|^2 \right\}. \quad (2.6)$$

Using above results the PAR can be computed easily. Assuming the same signal constellation on all tones reveals that PAR can be upper bounded by

$$PAR\{x^m[n/L]\} \leq N \frac{\max |X_k|^2}{E\left[\left| X_k \right|^2 \right]} \quad (2.7)$$

where equality is achieved for example at $n = 0$ when all QAM subsymbols have the same phase, i.e.

$$\arg\{X_0^m\} = \arg\{X_k^m\}, \quad k = 1, \dots, N-1. \quad (2.8)$$

2.5 PAR Reduction Methods

The PAR is considered as one of the major problem in the multicarrier communication systems and a large number of efforts have been put to solve this problem. A number of different PAR reduction approaches have been developed in the recent years. The different methods which are proposed can be categorized into several classes and in this section, summarizes different methods how to solve the PAR problem. Before going into details of different PAR reduction methods we look at the goal of PAR reduction. The goal of a PAR reduction algorithm is to lower the PAR as much as possible, while at the same time not disturbing other parts of the system. The complexity of the algorithm should not be too high and it should be easily implement able. We broadly define the two categories of PAR reduction methods.

2.5.1 Transparent Methods

Here the receiver does not require knowledge about the method applied by the transmitter. Similarly, the receiver can use a method unknown to the transmitter. These methods can be easily implemented in existing standards without any changes to existing specifications. This thesis focuses on a transparent method.

2.5.1.1 Clipping

This is one of the simplest ways to reduce the PAR in the OFDM system. In the clipping method we simply clip the high amplitude peaks. There are several clipping techniques which are described in the literature [4, 5]. Some of these techniques use digital clipping, i.e. the signal is clipped at the output of the inverse discrete Fourier transform without any oversampling. This causes re-growth of the signal peaks after the subsequent interpolation. To avoid the signal re-growth some techniques clip the signal after interpolation and then use a filter to reduce the resulting out-of-band spectral leakage. However the filters used in these techniques are complicated and computationally expensive. In addition they cause peak re-growth and result in significant distortion of the wanted signal [19]. The peak- windowing scheme presented in [2] is one of the clipping techniques that try to minimize the out of band distortion by using narrowband windows.

2.5.1.2 Tone Reservation

In the tone reservation method the orthogonality between the different subcarrier is exploited to generate the peak reduction signal. In the OFDM system not all subcarriers are used for data transmission. Some of them are reserved for the reduction signal. Due to

the fact that all subcarrier are orthogonal the signal generated by the reserved tones does not disturb the data carrying tones. In the tone reservation method both transmitter and receiver know the set of data carrying subcarriers. The construction of the reduction signal can be done in different ways with different complexities. The PAR reduction method using tone reservation method can be transformed into a convex optimization problem. This approach is used in this thesis. Advantages of tone reservation include among other no side information and low complexity.

2.5.1.3 Active Constellation Extension

The active constellation extension method proposed in [2, 12] is an extension of the tone injection method for PAR reduction. Here only the points at the constellation boundary have multiple representations and these points can be moved anywhere. The advantage with this method is that the decision regions for the receiver are not changing, so neither receivers nor the standard have to be changed. In systems that have very large constellations only a small part of the constellations is placed on the edges and there are fewer possibilities to move the points on the constellation boundaries, in these cases the reduction performance is low.

2.5.2 Non Transparent Methods

If the transmitter or the receiver incorporates a method to reduce PAR that requires side information to be transmitted from one side to the other. Majority of the PAR reduction algorithms are included in this category.

2.5.2.1 Coding Schemes

Different block coding methods can be used to reduce the PAR of OFDM system and different coding schemes are presented in [3] that uses well-known block codes with constant-modulus constellations, such as QPSK and M-PSK for PAR reduction purposes. The basic idea is that the block codes are used to remove some constellation combinations that produce large peaks and the encoded system will have smaller peaks than the uncoded system. One of the major drawbacks of this method is that it severely reduces data rate in order to achieve a good PAR reduction.

2.5.2.2 Phase Optimization Techniques

It was observed that we will get large PAR values when symbol phases in the subchannels are lined up in such a fashion that results in a constructive superposition forming a peak in the discrete time signal [2]. By rotating the channel constellations properly the peaks can be reduced. The partial transmit sequence [6] optimization scheme is such method. In partial transmit sequence the data carrying subcarrier blocks is further divided into disjoint carrier subblocks and then phase transformation (phase rotation) is applied for each subblocks. A number of iterations are required to find the optimum

phase rotation factor for different subblocks. Adaptive partial transmit sequence is proposed in [7] to reduce the number of iterations required to find optimum combination of factors for subblocks. Adaptive partial transmit sequence reduces the number of iteration by setting up a desired threshold and trial for different weighing factors until the PAR drops under the threshold.

Another method in this category is the selective mapping scheme [9]. In the selective mapping method one single data vector has multiple phase rotations, and the one that minimizes the signal peak is used. Information about which particular data vector and transformation was used is sent as side information to the receiver. In the presence of noise there can be a problem with decoding the signal.

2.5.2.3 Tone Injection

The tone injection method for PAR reduction is presented in [11]. The reduction signal also uses the data carrying tones, i.e. both the reduction as well as data carrying signal uses the same frequencies. But at the same time the constellation size is increased so that each point in the original basic constellation can be mapped into several equivalent points in the expanded constellation. On the receiver side the point is brought back to the original position by a modulo operation after the FFT.

This method is called tone injection because substituting the points in the basic constellation for the new points in the extended constellation is equivalent to inject a new tone of suitable frequency and phase in the multicarrier symbol. This method has a few drawbacks e.g. side information for decoding the signal is required on the receiver side and due to an extra IFFT operation it is more complex.

3 Tone Reservation

The tone reservation method for PAR reduction was proposed by Gatherer and Polley [13] and Tellado and Cioffi [11]. Both of these groups developed this approach independently and used projection of the signal peaks onto the reserved tones to generate the reduction signal. Reserving some tones for the peak reduction signal will lower the capacity but this loss in capacity is well spent to decrease PAR. The construction of the reduction signal based on the reserved tones can be done in different ways, with different complexities. The amount of peak-power reduction using tone reservation depends on four factors:

- Number of reserved tones
- Location of the reserved tones
- Amount of complexity
- Allowed power on reserved tones

Tone reservation method is an additive method because we introduce an additional signal $c^m[n]$, which is added to the original discrete time signal $x^m[n]$. The new composite signal can be formulated in the discrete time domain as

$$\bar{x}^m[n] = x^m[n] + c^m[n]. \quad (3.1)$$

The linearity property of the IFFT can be used to represent this addition in frequency domain as

$$\bar{X}^m[k] = X_k^m + C_k^m, \quad (3.2)$$

which results in the following relation:

$$\bar{x}^m[n] = \frac{1}{\sqrt{N}} \sum_{k=0}^{N-1} (X_k^m + C_k^m) \exp^{j2\pi kn/N} \quad (3.3)$$

The main purpose in the tone reservation method is to design the signal $c^m[n]$ so that we can reduce the peak power of a system. Design of $c^m[n]$ in time domain is very difficult because the data symbols are given in frequency domain. To simplify the design problem we design C_k^m in frequency domain. The tone reservation technique for PAR reduction affects both the average power of the signal and the signal peaks. However PAR after reduction is denoted as

$$PAR(x^m[n] + c^m[n]) = \frac{\max |x^m[n] + c^m[n]|^2}{E[|x^m[n]|^2]}. \quad (3.4)$$

This above definition of the PAR does not give the true peak to average ratio of the signal because the PAR defined here is a function of the signal before and after reduction. In above definition we have used the average power of the original signal because the average power is a simpler way of normalizing peak power results. This normalizing factor should remain constant for comparison purpose and with the restriction that the additive PAR reduction signal does not distort the data symbols this is very fair definition of PAR.

3.1 Problem Formulation

In this section the PAR reduction problem using tone reservation method will be formulated. A detailed mathematical derivation can be found in [2] and [11]. Most of the mathematics in this section and in the later section is taken from [2]. We start the formulation of the PAR reduction problem by considering an L times-oversampled version of the discrete time signal $x^m[n]$, i.e. $x^m[n/L]$. The main goal of the tone reservation method is to add a peak cancelling signal $c^m[n/L]$ to the original signal $x^m[n/L]$ to generate a lower peak power signal $\bar{x}^m[n/L]$. The peak cancelling signal $c^m[n/L]$ is generated through design of C_k^m the reserved tones. The matrix notation of $x^m[n/L]$ is

$$\begin{bmatrix} x_0^m \\ x_{1/L}^m \\ x_{2/L}^m \\ \vdots \\ \vdots \\ x_{n/L}^m \\ \vdots \\ \vdots \\ x_{(NL-1)/L}^m \end{bmatrix}_{NL \times 1} = Q \begin{bmatrix} X_0^m \\ X_1^m \\ 0 \\ \vdots \\ 0 \\ X_k^m \\ \vdots \\ \vdots \\ X_{N-1}^m \end{bmatrix}_{NL \times 1}, \quad (3.5)$$

where Q is the IDFT matrix of size NL but scaled by \sqrt{L} .

$$Q = \frac{1}{\sqrt{N}} \begin{bmatrix} 1 & 1 & \cdots & 1 \\ 1 & e^{j\frac{2\pi}{NL}1.1} & \cdots & e^{j\frac{2\pi}{NL}(NL-1)} \\ 1 & e^{j\frac{2\pi}{NL}2.2} & \cdots & e^{j\frac{2\pi}{NL}2(NL-1)} \\ \vdots & \vdots & \ddots & \vdots \\ 1 & e^{j\frac{2\pi}{NL}n.1} & \cdots & e^{j\frac{2\pi}{NL}n(NL-1)} \\ \vdots & \vdots & \ddots & \vdots \\ 1 & e^{j\frac{2\pi}{NL}(NL-1)} & \cdots & e^{j\frac{2\pi}{NL}(NL-1)(NL-1)} \end{bmatrix}_{NL \times N} \quad (3.6)$$

The multicarrier modulator including oversampling can be described by $\mathbf{x}_L^m = Q\mathbf{X}_L^m$. The vector \mathbf{X}_L^m contains $N(L-1)$ zeros that results in interpolation in time domain. If we remove the zero padded portion of \mathbf{X}_L^m and the corresponding columns in the \mathbf{Q} then the above matrix equation simplifies. Let \mathbf{Q}_L be the submatrix of \mathbf{Q} that is formed by selecting the first and last $N/2$ columns of \mathbf{Q} , then the oversampled IDFT operation can be expressed as

$$\begin{bmatrix} x_0^m \\ x_{1/L}^m \\ x_{2/L}^m \\ \vdots \\ \vdots \\ x_{n/L}^m \\ \vdots \\ \vdots \\ x_{(NL-1)/L}^m \end{bmatrix}_{NL \times 1} = Q_L \begin{bmatrix} X_0^m \\ X_1^m \\ \vdots \\ X_k^m \\ \vdots \\ \vdots \\ X_{N-1}^m \end{bmatrix}_{N \times 1}, \quad (3.7)$$

where \mathbf{Q}_L has dimension $NL \times N$. The additive PAR reduction equation (3.1) can be expressed in matrix notation as:

$$\begin{bmatrix} x_0^m \\ x_{1/L}^m \\ x_{2/L}^m \\ \vdots \\ \vdots \\ x_{n/L}^m \\ \vdots \\ \vdots \\ x_{(NL-1)/L}^m \end{bmatrix}_{NL \times 1} + \begin{bmatrix} c_0^m \\ c_{1/L}^m \\ c_{2/L}^m \\ \vdots \\ \vdots \\ c_{n/L}^m \\ \vdots \\ \vdots \\ c_{(NL-1)/L}^m \end{bmatrix}_{NL \times 1} = Q_L \begin{bmatrix} X_0^m \\ X_1^m \\ \vdots \\ X_k^m \\ \vdots \\ X_{(N-1)}^m \end{bmatrix}_{N \times 1} + Q_L \begin{bmatrix} C_0^m \\ C_1^m \\ \vdots \\ C_k^m \\ \vdots \\ C_{(N-1)}^m \end{bmatrix}_{N \times 1} \quad (3.8)$$

A simpler equation representation of above expression is

$$\bar{\mathbf{x}}_L^m = \mathbf{x}_L^m + \mathbf{c}_L^m = \mathbf{Q}_L (\mathbf{X}^m + \mathbf{C}^m) \quad (3.9)$$

In case of real-valued baseband signal both \mathbf{x}_L^m and \mathbf{c}_L^m must be real valued sequence, \mathbf{X}^m and \mathbf{C}^m must therefore possess the Hermitian symmetry properties.

3.1.1 PAR Reduction Signal for Tone Reservation

In the tone reservation method for PAR reduction both the transmitter and the receiver have knowledge about the reserved tone set for generating the PAR reduction signal. The reserved tones are not used for data transmission thus we restrict the reduction signal to a subspace orthogonal to data. Then on the receiver side the data vector \mathbf{X}^m and the PAR reduction signal vector \mathbf{C}^m can easily be separated because both of them are on different subcarriers. Let's define the set of R reserved tones as $\mathcal{R} = \{i_0, \dots, i_{R-1}\}$ that is used for generation of the peak compensation signal with this set and knowing that \mathbf{X}^m and \mathbf{C}^m do not use the same tone, we can say

$$X_k^m + C_k^m = \begin{cases} C_k^m, & k \in \mathcal{R} \\ X_k^m, & k \in \mathcal{R}^c \end{cases} \quad (3.10)$$

The symbol demodulation at the receiver is done in the frequency domain on a tone-by-tone basis. Then the reserved subcarriers can be discarded at the receiver, while the data carrying subcarriers are used to find the transmitted bit stream. However, the subcarriers orthogonality can be affected if transmitter, channel or receiver introduces any nonlinearity before symbol demodulation. Then the peak-cancelling signal could effect data decisions.

Let $\hat{\mathbf{C}}^m$ be the length R vector that is constituted by the elements of \mathbf{C}^m contained on the reserved tones, i.e. $\hat{\mathbf{C}}^m = [C_{i_0}^m, \dots, C_{i_{R-1}}^m]^T$. Similarly we define a matrix $\hat{\mathbf{Q}}_L$ which is a submatrix of \mathbf{Q}_L containing the columns with indices $\mathcal{R} = \{i_0, \dots, i_{R-1}\}$ i.e. $\hat{\mathbf{Q}}_L = [\mathbf{q}_{i_0, L}^{col} | \dots | \mathbf{q}_{i_{R-1}, L}^{col}]$.

Then we can write

$$\mathbf{c}^m = \mathbf{Q}_L \mathbf{C}^m = \hat{\mathbf{Q}}_L \hat{\mathbf{C}}^m. \quad (3.11)$$

Now we can rewrite equation (3.9) as

$$\bar{\mathbf{x}}_L^m = \mathbf{x}_L^m + \mathbf{c}_L^m = \mathbf{x}_L^m + \hat{\mathbf{Q}}_L \hat{\mathbf{C}}^m \quad (3.12)$$

The PAR of the m -th OFDM symbol \mathbf{x}^m before PAR reduction using the compact vector notation is defined as

$$PAR(\mathbf{x}^m) = \frac{\|\mathbf{x}^m\|_\infty^2}{E\left[|\mathbf{x}^m|^2\right]} \quad (3.13)$$

Similarly the PAR of the additive symbol can be defined as

$$PAR(\mathbf{x}^m + \mathbf{c}^m) = \frac{\|\mathbf{x}^m + \mathbf{c}^m\|_\infty^2}{E\left\{\left|\mathbf{x}^m\right|^2\right\}}. \quad (3.14)$$

In above expression the term in the denominator is not a function of the PAR reduction signal. The problem of minimizing the PAR of the combined signal is equivalent to calculate the value of $\mathbf{c}^{m,opt}$, or equivalently $\hat{\mathbf{C}}^{m,opt}$, that minimizes the maximum value of the peak or ∞ -norm of the additive symbol $\mathbf{x}^m + \mathbf{c}^m$. That can be expressed in an optimization problem as

$$\min_{\hat{\mathbf{C}}^m} \|\mathbf{x}^m + \mathbf{c}^m\|_\infty = \min_{\hat{\mathbf{C}}^m} \left\| \mathbf{x}^m + \hat{\mathbf{Q}}_L \hat{\mathbf{C}}^m \right\|_\infty \quad (3.15)$$

Above optimization problem is a convex one w.r.t. variables

$$\hat{\mathbf{C}}^m = [C_{i_0}^m \dots C_{i_r}^m \dots C_{i_{R-1}}^m]^T \quad [19].$$

The above relation can also be expressed as

$$\begin{aligned} & \min_{\hat{\mathbf{C}}^m} E \\ & \text{subject to: } \left\| \mathbf{x}^m + \hat{\mathbf{Q}}_L \hat{\mathbf{C}}^m \right\|_{\infty}^2 \leq E, \end{aligned} \quad (3.16)$$

where E represents the maximum magnitude of the peak reduced signal. It was mathematically proved in [11] that the above problem is a convex problem because it tries to minimize a linear constraint over an intersection of quadratic constraints on the variable $\hat{\mathbf{C}}^m$. The above formulation is for a complex baseband signal and can be classified as quadratically constrained quadratic program (QCQP) which is a special case of the convex problem [11].

3.1.2 Optimal Tone Reservation: Real-Baseband Case

In case of real-valued baseband signals above convex problem can be solved by linear programming and mathematics of the problem in this case is simpler. Considering a real-valued multicarrier signal, this requires real peak cancelling signals thus imposing complex conjugate symmetry on the vector \mathbf{C}^m . The following derivation is done for the case when N is even but can be easily modified if N is odd. When N is even valued C_k^m must satisfy $C_k^m = (C_{N-k}^m)^*$, $k = 1, 2, \dots, N/2 - 1$. If DC and tone $N/2$ are used then they must be real valued. Suppose we have a set of R tones

$$\mathcal{R} = \{i_0, i_1, \dots, i_{R/2-1}, N - i_{R/2-1}, \dots, N - i_0\}. \quad (3.17)$$

To simplify our derivation we are not using DC and $N/2$ tones. The peak-cancelling signal is then formulated as

$$\begin{aligned} c[n/L] &= \frac{1}{\sqrt{N}} \sum_{r=0}^{R-1} C_{i_r}^m \exp^{j2\pi i_r n / NL} \\ &= \frac{2}{\sqrt{N}} \sum_{r=0}^{R/2-1} C_{i_r, re}^m \cos(2\pi i_r n / NL) - C_{i_r, im}^m \sin(2\pi i_r n / NL), \end{aligned} \quad (3.18)$$

with $n = 0, \dots, NL-1$, and $C_{i_r, re}^m$ and $C_{i_r, im}^m$ are the real and imaginary parts of $C_{i_r}^m$, respectively. The above expression can be written in matrix form as

$$\begin{bmatrix} c_0 \\ c_{1/L} \\ c_{2/L} \\ \vdots \\ \vdots \\ c_{n/L} \\ \vdots \\ \vdots \\ c_{(NL-1)/L} \end{bmatrix}_{NL \times 1} = \overset{\vee}{\mathbf{Q}}_L \begin{bmatrix} C_{i_0, re}^m \\ C_{i_0, im}^m \\ C_{i_1, re}^m \\ C_{i_1, im}^m \\ \vdots \\ C_{i_r, re}^m \\ C_{i_r, im}^m \\ \vdots \\ C_{i_{R/2-1}, re}^m \\ C_{i_{R/2-1}, im}^m \end{bmatrix}_{2R \times 1} \quad (3.19)$$

where all elements in above matrices are real valued. $\overset{\vee}{\mathbf{Q}}_L$ denotes the $NL \times R$ matrix that includes all the sinusoidal terms, i.e.

$$\overset{\vee}{Q}_L(m, n) = \begin{cases} \frac{2}{\sqrt{N}} \cos(2\pi i_m n / NL), & m \text{ even} \\ \frac{2}{\sqrt{N}} \sin(2\pi i_m n / NL), & m \text{ odd} \end{cases} \quad (3.20)$$

Since we are dealing with only a single OFDM symbol block at a given time, the m superscript will be dropped to simplify notations in the remaining section.

For the real baseband case the minimax PAR problem, i.e. minimize the maximum peak magnitude to minimize PAR can be rewritten as

$$\begin{aligned} & \min_{\hat{\mathbf{c}}} E \\ & \text{subject to: } \left| x_{k/L} + \mathbf{q}_k \hat{\mathbf{C}} \right| \leq E \text{ for all } k = 0, 1, \dots, NL-1 \quad (3.21) \\ & \text{and } E \geq 0, \hat{\mathbf{C}} \in \Re^R, \end{aligned}$$

where \mathbf{q}_k represents the k th row of $\overset{\vee}{\mathbf{Q}}_L$ and $\hat{\mathbf{C}}$ represents the reordered tone coefficient vector in (3.19) [2].

The equation (3.21) can be easily converted into a linear program, which can be solved exactly. Converting (3.21) into a linear program results in

$$\begin{aligned}
 & \min_{\hat{\mathbf{c}}} \quad E \\
 & \text{subject to: } x_{k/L} + \mathbf{q}_k^{\vee} \hat{\mathbf{C}} \leq E \quad \text{for all } k = 0, 1, \dots, NL-1 \\
 & x_{k/L} + \mathbf{q}_k^{\vee} \hat{\mathbf{C}} \geq -E \quad \text{for all } k = 0, 1, \dots, NL-1 \\
 & \text{and } E \geq 0, \hat{\mathbf{C}} \in \mathfrak{R}^R.
 \end{aligned} \tag{3.22}$$

Now we will write these NL scalar constraints into a vector form and move all unknowns ($\hat{\mathbf{C}}$ and E) to the left hand side. The resulting linear program can be rewritten as

$$\begin{aligned}
 & \min_{\hat{\mathbf{c}}} \quad E \\
 & \text{subject to: } \mathbf{Q}_L^{\vee} \hat{\mathbf{C}} - E \mathbf{1}_{NL} \leq -\mathbf{x} \\
 & \mathbf{Q}_L^{\vee} \hat{\mathbf{C}} + E \mathbf{1}_{NL} \geq -\mathbf{x} \\
 & \text{and } E \geq 0, \hat{\mathbf{C}} \in \mathfrak{R}^R.
 \end{aligned} \tag{3.23}$$

The coefficients in $\hat{\mathbf{C}}$ are free variable (i.e. not required to be nonnegative) [2] so the above expression is not in the standard LP model form presented in [14]

Using the variable transformation $\hat{\mathbf{C}} = \hat{\mathbf{D}} - \hat{\mathbf{B}}$ the linear program can be converted into the standard linear program model.

$$\begin{aligned}
 & \min_{\hat{\mathbf{c}}} \quad E \\
 & \text{subject to: } \begin{pmatrix} \mathbf{Q}_L^{\vee} & -\mathbf{Q}_L^{\vee} & -\mathbf{1}_{NL} \\ -\mathbf{Q}_L^{\vee} & \mathbf{Q}_L^{\vee} & -\mathbf{1}_{NL} \end{pmatrix} \begin{pmatrix} \hat{\mathbf{D}} \\ \hat{\mathbf{B}} \\ E \end{pmatrix} \leq \begin{pmatrix} -\mathbf{x} \\ \mathbf{x} \end{pmatrix} \\
 & \text{and } E \geq 0, \hat{\mathbf{D}} \geq 0, \hat{\mathbf{B}} \geq 0
 \end{aligned} \tag{3.24}$$

In the above relation the vector inequality shows that each element of a vector is nonnegative, and the result is in the standard form of linear programming.

$$\begin{aligned}
 & \min \quad \mathbf{c}^T \mathbf{y} \\
 & \mathbf{A} \mathbf{y} \leq \mathbf{b} \\
 & \text{and } \mathbf{y} \geq 0
 \end{aligned} \tag{3.25}$$

To convert the inequalities to equalities we use the slack variable and following new program is obtained.

$$\begin{aligned}
 & \min_{\hat{\mathbf{c}}} \quad E \\
 & \text{subject to: } x_{k/L} + \mathbf{q}_k^{\vee} \hat{\mathbf{C}} + s_{k/l}^+ = E \quad \text{for all } k = 0, 1, \dots, NL-1 \\
 & x_{k/L} + \mathbf{q}_k^{\vee} \hat{\mathbf{C}} + s_{k/l}^- = -E \quad \text{for all } k = 0, 1, \dots, NL-1 \\
 & \text{and } s_0^+ \geq 0, s_1^+ \geq 0, \dots, s_{l-1}^+ \geq 0 \\
 & s_0^- \geq 0, s_1^- \geq 0, \dots, s_{l-1}^- \geq 0 \\
 & E \geq 0, \hat{\mathbf{C}} \in \mathfrak{R}^R,
 \end{aligned} \tag{3.26}$$

$s_{k/l}^+$ and $s_{k/l}^-$ are slack variables for positive and negative peak inequalities, respectively. They are constrained to be nonnegative in order to satisfy the original inequality constraints. When we add these slack variables to (3.24), we obtain

$$\begin{aligned}
 & \min_{\hat{\mathbf{c}}} \quad E \\
 & \text{subject to: } \begin{pmatrix} \mathbf{Q}_L^{\vee} & -\mathbf{Q}_L^{\vee} & -\mathbf{1}_{NL} & \mathbf{I}_N & \mathbf{0}_N \\ -\mathbf{Q}_L^{\vee} & \mathbf{Q}_L^{\vee} & -\mathbf{1}_{NL} & \mathbf{0}_N & \mathbf{I}_N \end{pmatrix} \begin{pmatrix} \hat{\mathbf{D}} \\ \hat{\mathbf{B}} \\ E \\ \mathbf{s}^+ \\ \mathbf{s}^- \end{pmatrix} = \begin{pmatrix} -\mathbf{x} \\ \mathbf{x} \end{pmatrix} \\
 & \text{and } s_0^+ \geq 0, s_1^+ \geq 0, \dots, s_{l-1}^+ \geq 0 \\
 & s_0^- \geq 0, s_1^- \geq 0, \dots, s_{l-1}^- \geq 0 \\
 & E \geq 0, \hat{\mathbf{D}} \geq 0, \hat{\mathbf{B}} \geq 0,
 \end{aligned} \tag{3.27}$$

where \mathbf{I}_N and $\mathbf{0}_N$ are $N \times N$ identity and zero matrices, respectively. \mathbf{x} is a vector representation of OFDM symbol. This problem is now in the form that represents the standard form a linear program, i.e.

$$\begin{aligned}
 & \min \quad \mathbf{c}^T \mathbf{y} \\
 & \text{subject to: } \mathbf{A} \mathbf{y} = \mathbf{b} \\
 & \text{and } \mathbf{y} \geq 0
 \end{aligned} \tag{3.28}$$

In the above equation \mathbf{y} are the optimization variables, matrix \mathbf{A} , and the vectors \mathbf{b} and \mathbf{c} are known parameters.

When we compare the standard form in (3.28) to (3.27) we see that matrix \mathbf{A} has the dimensions $2NL \times (2NL + 2R + 1)$, the length of vector \mathbf{y} is $(2NL + 2R + 1)$, and the vector \mathbf{b} has a length of $2NL$. To find the optimal solution linear programming theory can be applied directly to the minimax PAR reduction problem.

3.1.3 Optimal Tone Reservation: Complex-Baseband Case

In section 3.1.1 where we have formulated the minimax PAR problem we have observed that for complex baseband signals the problem is a quadratically constrained quadratic program (QCQP). In this case the constraints are absolute values of complex variables which can be translated into quadratic constraints. The function to minimize is linear. Solving this quadratically constrained quadratic program directly for complex baseband signal is very difficult and costly. In [1] and [19] a method of complex base band approximation is presented which converts this quadratically constrained quadratic program into a linear program. All the mathematics we have derived above will be then valid for the complex baseband case. Since we use an approximation the derived solution is only suboptimal.

The main goal of PAR reduction is to minimize the PAR level as much as possible. For the real baseband case we try to minimize the value of additive signal $\mathbf{x}^m + \mathbf{c}^m$ on the real axis. For the complex baseband signal, the minimax PAR optimization problem occurs in the complex plane and we have to minimize the maximum distance of the additive signal $\mathbf{x}^m + \mathbf{c}^m$ from the origin. Minimizing the maximum distance of $\mathbf{x}^m + \mathbf{c}^m$ from the origin is equivalent to minimizing the radius of a circle that constrains all values of $\mathbf{x}^m + \mathbf{c}^m$ [2]. The resulting problem can be solved efficiently by a complex FIR filter design technique presented in [17] where the circular boundaries are approximated. The same approach is applied here by splitting the imaginary and real coefficients of the complex sample into two separate real signals. Then the same approach as for the real baseband optimization is applied, i.e. to minimize the maximum magnitude of these coefficients. This approach of treating the complex valued samples as two real signals and then minimizing there maximum magnitude is equivalent to constrain the magnitude of all samples into a square boundary in the complex plane.

This suboptimal approximation helps us to write a linear program with twice the number of constraint equations as we have in the real baseband case. In practical systems this square approximation of the circle is not sufficient and we have to use higher order approximation. One such approximation to the circle is the octagon. If we rotate the phase of all the samples in time domain by $\pi / 4$ we get a new set of real and imaginary coefficients. These new $\pi / 4$ -phase rotated versions of coefficients are correlated to the original real and imaginary coefficients. Imposing our goal of minimizing the maximum magnitude of samples on the original and $\pi / 4$ - phase rotated coefficients, is equivalent to constrain the original signal $\mathbf{x}^m + \mathbf{c}^m$ within an octagon. This new problem can be written as a linear program with four times more constraint equations than for the real

baseband case. We can use further phase rotations like 16-agon, 32-agon, and large boundaries. As we go for larger boundaries to better approximate a circle the complexity of the problem increases as the no of constrained equation increases each time. The approximation can be quantified by the maximum magnitude outside of the circle. For the square, octagonal and 16-agonal approximations the maximum peak increase outside of the circle is 3, 0.68, and 0.16dB, respectively.

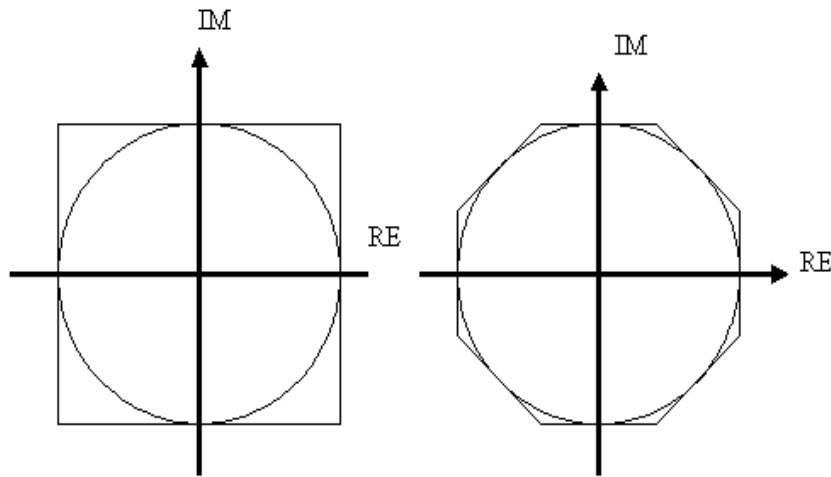


Figure 3.1: Approximation of a circle with a square and octagonal boundary.

4 Tone Reservation Kernel Design

Most of the tone reservation approaches uses some sort of iterative algorithms to reduce the high peaks. The performance of these algorithms depends a lot on the design and the properties of the tone reservation kernel \mathbf{p} . Usually in the tone reservation approach algorithms for PAR reduction the peak reduction kernel \mathbf{p} and the set of reserved tones \mathcal{R} are set during the initialization phase and remain then constant for all symbols. There are a number of approaches for choosing the tone reservation set since the location of the tones effects the overall PAR reduction gain. One common criteria to choose the reserved tones is to minimize the side lobes of tone reservation kernel \mathbf{p} . In this work this criteria is used. Once we have a set of reserved tones then for optimal performance the peak reduction kernel \mathbf{p} should be equal to the impulse, i.e. $[10\dots0]^T = \mathbf{e}_0$. If we design our kernel in this way then every time the tone reservation algorithm cancels a peak in the given symbol, secondary peaks are not generated at other locations [11]. However this kernel requires N coefficients in frequency domain, i.e. no tones are left for data transmission. Therefore we try to design a tone reservation kernel as close to \mathbf{e}_0 as possible and yet satisfy the condition $R \ll N$. The different solutions that are proposed for the design of the kernel \mathbf{p} depend on the chosen cost function to weight the similarities between \mathbf{p} and \mathbf{e}_0 , i.e. $d(\mathbf{p}, \mathbf{e}_0)$. A typical choice for $d(\cdot, \cdot)$ is a l - norm, i.e. $d(x, y) = \|x - y\|_l$. When $l=2$ we get the Mean Square Error (MSE) solution. When $l=1$ and $l=\infty$, the tone reservation kernel design problem can be solved by a linear program provided that we have a real baseband signal, and by QCQP when we have a complex baseband signal [11].

Let the nonzero values of \mathbf{P} be denoted by $\hat{\mathbf{P}}$, i.e. $\hat{\mathbf{P}} = [P_{i_0} \dots P_{i_{R-1}}]^T$, where \mathbf{P} is the frequency domain representation of the peak reduction kernel \mathbf{p} . The simplest way to choose the tone reservation kernel $\mathbf{p} = \hat{Q}_L \hat{\mathbf{P}}$ is to use the MSE criterion, i.e.

$$\hat{\mathbf{P}}^{\|2} = \arg \min_{\hat{\mathbf{P}}} \left\| \hat{Q}_L \hat{\mathbf{P}} - \mathbf{e}_0 \right\|_2 \quad (4.1)$$

and

$$\mathbf{p}^{\|2} = \hat{Q}_L \hat{\mathbf{P}}^{\|2} \quad (4.2)$$

This case gives us a simple closed form solution i.e.

$$\hat{\mathbf{P}}^{\|2} = \left(\hat{Q}_L^* \hat{Q}_L \right)^{-1} \hat{Q}_L^* \mathbf{e}_0 = \hat{Q}_L^* \mathbf{e}_0 \quad (4.3)$$

$$\hat{\mathbf{P}}^{\parallel 2} = \frac{1}{L\sqrt{N}} [1 \dots 1]^T = \frac{1}{L\sqrt{N}} \mathbf{1}_R \quad (4.4)$$

Thus, the MSE kernel is

$$\mathbf{p}^{\parallel 2} = \frac{1}{\sqrt{N}} \hat{Q}_L \mathbf{1}_R \quad (4.5)$$

Since we want $p_0 = 1$ so scale the kernel:

$$\hat{\mathbf{P}}^{\parallel 2} = \frac{\sqrt{N}}{R} \mathbf{1}_R \quad (4.6)$$

$$\mathbf{p}^{\parallel 2} = \frac{\sqrt{N}}{R} \hat{Q}_L \mathbf{1}_R \quad (4.7)$$

The MSE kernel $\mathbf{p}^{\parallel 2}$ obtained from (4.7) has a straightforward closed form solution and its design requires NR multiplies and adds. The MSE kernel $\mathbf{p}^{\parallel 2}$ only depends on the reserved tone set \mathcal{R} . Therefore the kernel only needs to be computed if there is a change of the peak reduction tone location. The MSE kernel can be implemented efficiently. The algorithm for the MSE kernel computations becomes a part of the tone reservation algorithm. The MSE kernel is computed during initialization of the tone reservation algorithm to achieve maximum performance.

The following algorithm which is presented in [11] can be used to compute the MSE kernel.

1. We choose a set of R random locations over the interval $(0, \dots, N-1)$ to generate the tone reservation set and this set of indices is represented as $\mathcal{R} = \{i_0, \dots, i_{R-1}\}$.
2. Now we set the value of the R reserved tones to \sqrt{N}/R , and the remaining $N-R$ tones values are set to zero, i.e. $P[k] = \sqrt{N}/R$, for $k \in \mathcal{R}$, $P[k]=0$, for $k \notin \mathcal{R}$.
3. An IFFT operation is performed to compute $p[n] = IFFT(P[k])$ and the largest value will be at $p[0]$.
4. The secondary peak of $p[n]$ is computed, i.e. $\max\{|p[n]|\}$ for $n \in \{1, \dots, (N-1)\}$.
5. Choose a new tone set and back to 1.

5 Active-Set Methods

Before discussing the active-set algorithm we will look at the basic principle of active set methods and how they work. Generally active-set methods are useful for the optimization problem of the form:

$$\begin{aligned} \text{minimize: } & f(x) \\ \text{subject to: } & g_i(x) \leq 0, \quad i = 1, 2, \dots \end{aligned} \quad (5.1)$$

Here we define an inequality constraint $g_i(x) \leq 0$ as active at a feasible point x if $g_i(x) = 0$ and inactive at x if $g_i(x) < 0$. The fundamental idea behind the active-set methods presented in [14] is that we divide the inequality constraints into two groups, one of the groups contains the inequality constraints that are active and the other group contains those that are treated as inactive. The goal is to determine the active set $A(x')$ for a local minimum for the given test point x' so that the necessary Kuhn-Tucker conditions are satisfied. These necessary conditions state that there exist a μ that satisfies

$$\begin{aligned} \nabla f(x') + \sum_{i \in A(x')} \mu_i \nabla g_i(x') &= 0, \\ \mu_i &\geq 0 \quad \text{for all } i \in A(x') \\ \mu_i &= 0 \quad \text{for all } i \notin A(x'). \end{aligned} \quad (5.2)$$

The Lagrange multipliers must be zero for the inactive constraints. In order to see if (5.2) is satisfied μ_i 's associated with active constraints are checked and if they are nonnegative then we are fulfilling the conditions listed in 5.2.

Let's define a working set as a set of constraints that are active at the current point or it may be a subset of these constraints that are active at that point. So at every iteration of the active-set algorithm a working set is defined and it is considered as the active set. The algorithm then tries to move on the working surface until it reaches at an improved feasible point which may offer new additions to the active set [2]. The working surface is defined by the working set. This process is repeated until we reach on an optimal or suboptimal solution.

If we have finite number of constraints then the basic active-set method presented in [14] converges to the optimal solution in a finite number of iterations.

6 Practical Active-Set Tone Reservation

In this section we will discuss the practical active-set algorithm which is used for PAR reduction in the OFDM system. To find the exact optimal PAR reduction solution is computationally expensive and it is not suitable to be used in a real time system. So for practical purposes we use a suboptimal solution of the PAR reduction problem that yields satisfactory performance and relatively low computational complexity. The active set algorithm for PAR reduction was first presented by Brian S. Krongold and detailed work is present in [2]. First of all we will look at the active-set algorithm for the real baseband case and later we will extend it for complex baseband signals. As stated in [19] in order to implement the active-set algorithm for real baseband signals two algorithmic needs must be focused. These are

- How to determine the active set descent direction
- How to determine the next active constraints, i.e. the next peak in the active set.

6.1 Determining Descent Direction

According to basic the principal of the active-set method when we have a working surface also known as feasible region then while moving through this working surface the current active constraints must remain active. In the PAR reduction problem the largest peaks in the symbol form the active constraints so keeping the current constraints active is equivalent to keeping the current largest peaks balanced at the same amplitude. The peak reduction update at the i th iteration of the active set iteration can be written as:

$$\bar{x}^{(i+1)} = \bar{x}^i - \mu^i \bar{\mathbf{p}}^i, \quad (6.1)$$

where in above update equation \bar{x}^i is the time domain signal block at the i th iteration, $\bar{\mathbf{p}}^i$ is the descent direction in the i th iteration, and μ^i represents the distance travelled in the descent direction.

When we have i peaks that are balanced at locations n_1, n_2, \dots, n_i , and we are at the start of i th iteration then in order to keep these peaks balanced while moving through the descent direction the following property must be satisfied:

$$\bar{p}_{n_j}^i = \text{sign}(\bar{x}_{n_j}^i), \quad j = 1, 2, \dots, i \quad (6.2)$$

We assume that the peak reduction kernel is scaled so that it has unit magnitude at the origin. When we fulfil this condition then no matter what value of μ we choose the magnitudes of the peaks which we have already balanced at n_1, n_2, \dots, n_i will remain balanced.

To reduce a peak at any location n the peak reduction kernel is circularly shifted by n to generate a new signal \mathbf{p}_n and this new signal is used to reduce that peak. For every

sample of the active set \mathbf{p}_{n_i} can be used to reduce its magnitude. In order to satisfy the constraints in (6.2) a linear combination of shifted versions of the peak reduction kernel \mathbf{p}_0 is generated. The formula to calculate $\bar{\mathbf{p}}^{-i}$ is written as

$$\bar{\mathbf{p}}^{-i} = \sum_{k=0}^i \alpha_k \mathbf{p}_{n_k} . \quad (6.3)$$

The following $i \times i$ system of equations needs to be solved in order to determine the necessary α weights [2]:

$$\begin{bmatrix} 1 & p(n_1 - n_2) & \cdots & p(n_1 - n_i) \\ p(n_2 - n_1) & 1 & \cdots & p(n_2 - n_i) \\ \vdots & \vdots & \ddots & \vdots \\ p(n_i - n_1) & p(n_i - n_2) & \cdots & 1 \end{bmatrix} \begin{bmatrix} \alpha_1 \\ \alpha_2 \\ \cdots \\ \alpha_i \end{bmatrix} = \begin{bmatrix} S_{n_0} \\ S_{n_1} \\ \vdots \\ S_{n_i} \end{bmatrix} . \quad (6.4)$$

The equation system at the i th iteration can be solved for α weights by determining $i \times i$ matrix inverse and multiplying the right hand side vector with this matrix inverse. The size of the square matrix in above relation is equal to the iteration number in the active set algorithm. If we assume that the prototype signal \mathbf{p}_0 is a symmetric function this matrix will also be a symmetric matrix and we can use techniques to find the inverse that takes this into account [18]. This will increase the computational efficiency.

6.2 Determining the Signal Next Active Constraint

At every iteration of the active-set algorithm the peak reduction kernel is circularly shifted to reduce active peaks equally. The next goal is to reduce them until the point that another peak is balanced and joins active set. This active peak represents a new active constraint in the active-set. To achieve this it requires that we determine a μ^{i*} that balances the active peaks at n_1, n_2, \dots, n_i and the new peak at n_{i+1} . A new peak must not produce a magnitude that is greater than the magnitude of the active peaks in the active set or in other words we can say that the balanced peaks must represent the maximum magnitude in \bar{x}^{-i+1} . For every sample k that is not part of the active set, there will be some positive step size μ_k^i that balances the active peaks and \bar{x}_k^{-i+1} at some magnitude $E_k^{i+1} = E^i - \mu_k^i$. However, the reduction of magnitude of this sample may increase the magnitude of other samples which may become larger than E_k^{i+1} . This violates the concept of active-set approach. This situation can be avoided by using the fact that each OFDM symbol is a deterministic signal, so each sample k that is not part of active set is tested to determine the value of step size μ_k^i that causes a balance at

magnitude E_k^{i+1} . The parameters, which are required to find this, are \bar{x}_k^i , E^i , and \bar{p}_k^i . The balancing may occur at E_k^{i+1} or $-E_k^{i+1}$, because we are dealing with magnitude, and E is strictly nonnegative. So the equations for the positive and negative balancing are

$$\text{positive balancing : } E_k^{i+1} = E^i - \mu_k^{i+} = \bar{x}_k^i - \mu_k^{i+} \bar{p}_k^i, \quad (6.5)$$

$$\text{negative balancing : } -E_k^{i+1} = -(E^i - \mu_k^{i-}) = \bar{x}_k^i - \mu_k^{i-} \bar{p}_k^i. \quad (6.6)$$

When we solve for $\mu^i + k$ using the right-most equalities on both of above equations, we obtain the following:

$$\text{positive balancing : } \mu_k^{i+} = \frac{E^i - \bar{x}_k^i}{1 - \bar{p}_k^i} \quad (6.7)$$

$$\text{negative balancing : } \mu_k^{i-} = \frac{E^i + \bar{x}_k^i}{1 + \bar{p}_k^i}. \quad (6.8)$$

We are only interested in positive values of μ_k^i since a negative step size increases the peak power.

The optimal balancing point can be easily determined by increasing μ from 0 until to a point where a new peak balances with the previous peaks. Any value of μ greater than this optimal value will not produce a peak larger than the balanced peaks, and no values of μ below this value cause a new active constraint. Therefore if we are testing all possible sample k that do not lie in the active set of peaks, the μ_k that has the minimum positive value will be the optimal step size. This optimal step size will add the next constraint to the active set:

$$\mu^{i*} = \min\{\mu_k^{i+}, \mu_k^{i-} : k \notin W, \mu_k^{i+} \geq 0, \mu_k^{i-} \geq 0\}, \quad (6.9)$$

W represents the set of samples in the active set.

To find the optimal step size by testing all samples that do not lie in the active set of the peaks is computationally intensive. But complexity reduction techniques presented in [14] can be used to reduce this complexity. The details of these techniques which we apply during our simulations can be found in [2] and are also described here. As stated in [19] this technique is a simple sign balancing assumption which is valid for early stages of active-set approach with N being large. The assumption is that if \bar{x}_k^i has a positive value then it is unlikely that the negative balancing step size is optimal and vice versa for the positive values of \bar{x}_k^i . This assumption reduces the testing of each sample to either a negative or positive peak balance testing and we only need to evaluate the following:

$$\mu^{i*} = \min_{k \in W} \left(\frac{E^i - |x_k^{-i}|}{1 - \text{sign}(x_k^{-i}) p_k^{-i}} \geq 0 \right) \quad (6.10)$$

6.3 Complete Active-set Algorithm

The complete active set algorithm (from [19]) for real base band signals is summarized below with the assumption that the algorithm starts with x and the prototype function \mathbf{p}_0 .

1. We start the algorithm with $\bar{x}^{-1} = x$ and set iteration number to equal 1, i.e. $i = 1$. Let E_1 be the maximum magnitude sample and the active-set contains this maximum magnitude sample.
2. Set $\bar{\mathbf{p}}^{-1} = \mathbf{p}_0$.
3. Test all peaks with \bar{x}^{-i} and $\bar{\mathbf{p}}^{-i}$.
4. Find the optimal step size, i.e. minimum μ^i , and calculate $E^{i+1} = E^i - \mu^i$. Now the peak associated with this optimal step size μ^i will be added to the active set.
5. Calculate the peak reduced signal $\bar{\mathbf{x}}^{-i+1} = \bar{\mathbf{x}}^{-i} - \mu^i \bar{\mathbf{p}}^{-i}$.
6. If the maximum number of iterations is reached or a desired peak-power level is reached, then STOP.
7. Find the α values in (6.3) by solving the matrix equation.
8. Generate $\bar{\mathbf{p}}^{-i+1} = \sum_{k=0}^i \alpha_k \mathbf{p}_{n_k}$ where n_0, n_1, \dots, n_i represent the active peaks and go to STEP 3.

6.4 Extension to the Complex-Baseband Case

We have discussed earlier that the minimax PAR reduction problem in the complex baseband case can be solved by linear programming techniques when using a complex approximation. So to apply the active-set algorithm to the complex base band signal few adjustments are necessary to above real baseband active-set algorithm. In this section we present the adjustments for the octagonal symmetry. Extensions to higher order approximations are straight forward. In the octagonal approximation we are using a phase rotation of $\pi/4$ so first of all the signal \bar{x}^{-i} will be written as a series of real and imaginary parts of the signal that are phase shifted by 0 and $\pi/4$, respectively. In the real baseband case the peak reduction kernel is calculated by projecting an impulse at $n = 0$ on the reserved tones. For octagonal boundary four different impulses for either the real or imaginary coefficients and for either phase rotation will occur. The effect of these four

impulses will be projected onto both the original real-imaginary basis and the $\pi/4$ -rotated real-imaginary basis. By pre-compute and store the projections of $\delta(n)$, $j\delta(n)$, $e^{j\pi/4}\delta(n)$, $je^{j\pi/4}\delta(n)$ onto the reserved tones with respect to the original and $\pi/4$ phase rotated bases four different peak reduction kernel will be formed.

7 PSD constrained Tone reservation

So far we have discussed the optimization algorithm without any constraints on the different tones. However, in practical systems different constraints apply. In this section we will describe the PSD constrained on the reserved tones. When we solve the minimax PAR problem formulated in (3.21) the power on the reduction tones grows greatly in many cases. In practical systems the data tones must fulfil certain PSD constraints, which mean that we are not allowed to transmit unlimited power on these tones. Similar rules may apply on the reserved tones. When the power on the different tones is restricted then this effects the optimization problem which we have formulated in the previous section. The minimax PAR optimization problem is reformulated here for PSD constraint case.

The peak reduction signal $c^m[n/L]$ can be expressed as $\mathbf{c}^m = \mathbf{Q}_L^{\vee} \mathbf{C}^m$, where \mathbf{Q}_L^{\vee} is a matrix of sinusoidal and cosinusoidal column vector with frequencies specified by the R reserved tones t_1, t_2, \dots, t_R . \mathbf{C}^m is vector that contains the weight of these (co)sinusoids. Since we are dealing with only a single OFDM symbol block at a given time, the m superscript will be dropped to simplify notations.

The PSD constraints that limit the power on the reserved tones appear as quadratic constraints on the pair of sine and cosine components of the tone and they can be written as [1]

$$\mathbf{C}^T \begin{bmatrix} \mathbf{I}_l & \mathbf{0} \\ \mathbf{0} & \mathbf{I}_l \end{bmatrix} \mathbf{C} \leq A_l^2 \quad l = 1 \dots R, \quad (7.1)$$

where \mathbf{I}_l is the identity matrix of size R and A_l is the maximum amplitude of the reduction tone l . For the real baseband case the optimization problem in (3.21) can be written as [18]:

$$\begin{aligned} & \min_{\hat{\mathbf{c}}} \quad E \\ & \text{subject to: } \begin{cases} \mathbf{x}_L + \mathbf{Q}_L^{\vee} \mathbf{C} \leq E \\ -\mathbf{x}_L - \mathbf{Q}_L^{\vee} \mathbf{C} \leq E \end{cases} \end{aligned} \quad (7.2)$$

The optimization problem with PSD constraints included can be written as:

$$\begin{aligned} & \min_{\hat{\mathbf{c}}} \quad E \\ & \text{subject to: } \begin{cases} \mathbf{x} + \mathbf{Q}_L^{\vee} \mathbf{C} \leq E \\ -\mathbf{x}_L - \mathbf{Q}_L^{\vee} \mathbf{C} \leq E \\ \mathbf{C}_{(2l-1)}^2 + \mathbf{C}_{(2l)}^2 \leq A_{l,\max}^2 \end{cases} \end{aligned} \quad (7.3)$$

$A_{l,\max}$ is the amplitude limitation on the tone t_l . This problem is again quadratically constrained quadratic program.

To solve the optimization problem with linear programming algorithms, the constraints in the problem have to be linear. This requirement can be fully filled by a linear approximation of the quadratic constraint which transforms the QCQP problem into a linear program. Again the linear approximation of the constraining circle in the complex plane will be used. Figure 7.1 shows the linear approximation of the quadratic magnitude constraint. The circle in the figure represents the ideal power constraint and the octagon is used to implement a linear approximation. The octagon uses eight linear constraints to describe the circle. Polygons with a large number of sides can be used for a better approximation at the cost of a larger number of constraints in the linear program.

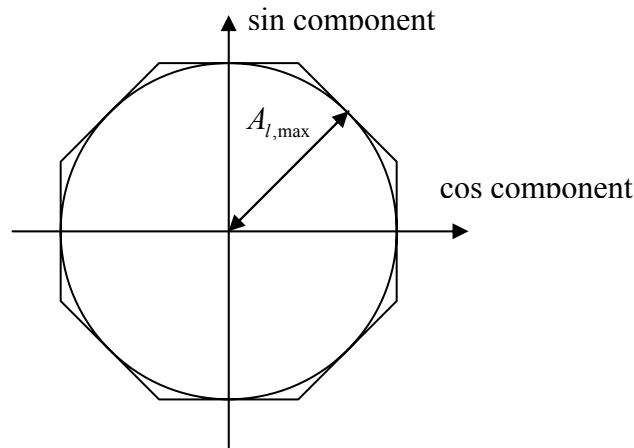


Figure 7.1: Linear approximation of quadratic constraints.

The value of the PSD constraint applied to the reduction tones has a great impact on the performance of the PAR reduction method. When the PSD constraint on the reserved tones is rather restrictive, then in some cases it is difficult to achieve good PAR reduction. If we have a small number of reserved tones for generation of the peak reduction signal and all these tones must fulfil the PSD constraint, then the largest reduction signal, which we can generate, is possible when all tones are placed in phase at a given sample. The reduction signal generated in this way will have one high peak and the height of this peak will be equal to the sum of the maximum amplitudes of the reserved tones. This will serve as a performance bound because if the difference between any data sample (having large peak) and the desired PAR level is larger than this, then it is not possible to reduce that sample down to the desired PAR level.

Let A_l be the maximum amplitude of reduction tone l . The constraint of maximum power per tone is equivalent to a constraint on the maximum magnitude. This constrained results in a limit on the magnitude of the peak reduction signal i.e.

$$A_{l,\max} = \sum_{l=1}^R A_l \quad l = 1, \dots, R, \quad (7.4)$$

where R denotes the number of tones reserved for PAR reduction.

So we can assume that an arbitrary reduction signal $c[n]$ can be generated with the limitation that it nowhere can have a value that is greater than the sum of the amplitudes of the reserved tones, i.e.

$$|c[n]| \leq A_{l,\max} = \sum_{l=1}^R A_l. \quad (7.5)$$

If we use this PSD bound then we can reduce all samples in the original signal $x[n]$ down to clip level $E\sigma$ provided that $|x[n]| \leq E\sigma + A_{l,\max}$. This PSD bound is less strict as compare to a PSD constraint on each tone.

The maximum tone amplitude $A_l(i)$ is proportional to σ , the standard deviation of the transmitted signal and can be calculated using the formula [1]:

$$A_l = \sigma \cdot \frac{\sqrt{2}}{\sqrt{R_o - R}} \cdot \frac{1}{\cos \frac{\pi}{s}} \quad (7.6)$$

The cosine expression $\cos(\pi/s)$ factor in the linear approximation of the power constrained, and R_o is the total number of the available tones for transitions. The above expression is independent of l and gives a constant valued PSD constrained on all reserved tones.

8 PSD-constrained active-set approach

In the active set algorithm presented in the previous Section 6 we have not considered any PSD constraint on the reserved tones used for the generation of peak reduction signal. If the active set algorithm is to be used in the PSD constrained case, it needs some modifications. To find the appropriate modification we first discuss three main outcomes when we perform an active set iteration on the PSD constraints tone set.

1. A new peak is balanced and no PSD constraints are met. This means that all reserved tones have amplitude less than the imposed PSD constraint. This is the same case as with no PSD constraint.
2. A new peak is balanced and before second active peak is encountered all reserved tones meet/exceed the PSD constraints at the same time.
3. Two or more peaks are balanced and before balancing a new peak some tones meet/exceed the PSD constraint while other tones are still available for further reduction.

For case 1, the algorithm will be identical to the non PSD constrained algorithm. When a new peak is balanced and no PSD constraints are met the algorithm can continue with its next iteration until the maximum number of iteration is reached or the desired PAR is achieved. For case 2, the algorithm stops at that point because this is the optimal point and moving beyond this point will violate the PSD constraint. So for case 2, the algorithm simply takes the step size μ_{\max} , this is the step size that fills all subchannels to the PSD constraint, and it stops here because the optimal solution has been reached [18].

Adding the tone weights to reduce two different peaks may cause the PSD constraints to be reached on certain tone while not on others. This is what happens in case 3 and is shown in the Figure 7.2

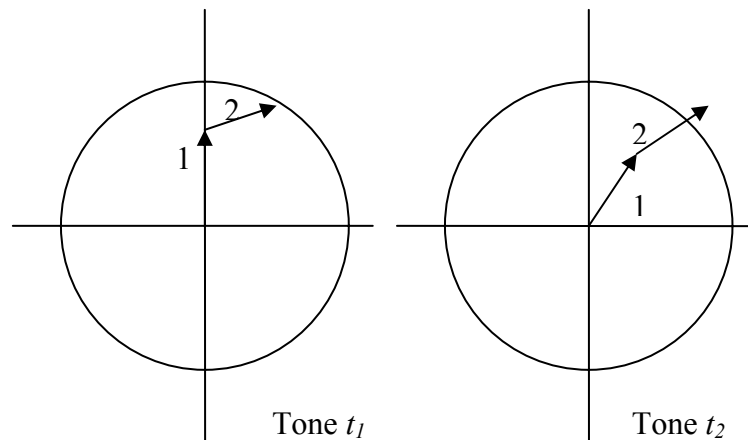


Figure 7.2: Addition of the tone weights for the reduction of two different peaks.

In case 3, the μ descent is scaled back to a point where the PSD constrained is met on a first tone. This tone is then frozen and can not be used for subsequent PSD reductions. The remaining tones which have not yet met PSD constraints can be used for the remaining iterations. This process is repeated until all reserved tones reaches their PSD constraint level or desired PAR level is achieved [18].

Now we will derive an expression to calculate the scaling factor for the μ descent.

Suppose \hat{C}_l represents the l th element of $\hat{\mathbf{C}}$, the total weight on tone t_l after i iterations. It can be formulated as

$$\hat{C}_l^{(i)} = \hat{C}_l^{(i-1)} + \Delta \hat{C}_l^{(i)}. \quad (8.1)$$

After each iteration the increments $\Delta \hat{C}_l^{(i)}$ include the effect from reducing one additional peak and we can express the increments $\Delta \hat{C}_l^{(i)}$ in cosine and sine components as [18]

$$\Delta \hat{C}_l^{(i)} = \begin{bmatrix} \Delta \hat{C}_{l,\cos}^{(i)} & \Delta \hat{C}_{l,\sin}^{(i)} \end{bmatrix} \quad (8.2)$$

$$\Delta \hat{C}_l^{(i)} = K \mu^i \sum_{k=0}^i \alpha_k^{(i)} \left[\cos\left(\frac{2\pi l n_k}{NL}\right) \quad \sin\left(\frac{2\pi l n_k}{NL}\right) \right] \quad (8.3)$$

where K is a constant that results from normalizing peak reduction kernel \mathbf{p} so that $p_0 = 1$. When active set algorithm is used together with PSD constrain then during each iteration, a new peak reduction signal $\bar{\mathbf{p}}^i$ is created and in parallel to that, the weight on each tone and the increments $\Delta \hat{C}_l^{(i)}$ are calculated. The quadratic equation

$$\left| c_l^{(i-1)} + \beta_l \mu^i \Delta c_l^{(i)} \right|^2 = A_{l,\max}^2 \quad (8.4)$$

is solved to find β_l and the smaller β_l value is chosen. Where β_l represents the scaling factor for μ^i . The tone powers are checked against the PSD constraint and if any of the tones exceeds the PSD constraint this minimum β_l is used to scale back μ^i . This modified step size is used to compute the final PAR reduction signal. The process is repeated whenever a tone reaches its PSD constraint.

9 Simulation and Results

The results of the simulations are presented in this section. First simulation methodology and selection of different parameters for active-set method will be discussed. Then results and different analysis will be presented.

To implement active set approach for PAR reduction of a complex baseband signal we generated complex baseband OFDM symbols of length 256, 512, 1024, and 2048 samples with 151, 301, 601, and 1201 tones are used for data transmission and PAR reduction signal generation, respectively (these system parameters are the same for downlink 3GPP transmission). Each of the data carrying tones uses a 16-point QAM constellation with average power equal to one.

Position of reserved tones for generation of PAR reduction signal is an important parameter in the active set approach. Previous results in [16] suggest that randomly selected tones give better results than block placed or equally spaced placed tones. In our simulation 10000 randomly selected tone sets are generated. Minimization of secondary peaks of peak reduction kernel is used as optimization criteria for selecting the optimal tone set. After determining the optimum tone set, the peak reduction kernel is generated by projecting an impulse at $n = 0$ onto the set of reserved tones. The projection of an impulse onto the reserved tone set is equivalent to least square approximation of the impulse with equal weight on all reduction tone. Figure 9.1 shows the magnitude of the peak reduction kernel generated from projecting an impulse on 26 randomly selected tones for a symbol of length 512.

The results of PAR reduction in the simulations are presented as the Complementary Cumulative Density Function (CCDF) of the PAR of the OFDM signals. The CCDF of PAR of an OFDM signal is expressed as follows:

$$CCDF(PAR(x)) = \text{Pr ob.}(block\ PAR(x) > E) \quad (9.1)$$

This equation can be read as the probability that at least one peak with in the symbol block is greater then some clip level E .

Similarly the sample PAR CCDF for an OFDM symbol is defined as:

$$CCDF(PAR(x_i)) = \text{Pr ob.}(sample\ PAR(x_i) > E), \quad (9.2)$$

where x_i represents a sample in a OFDM symbol of length N .

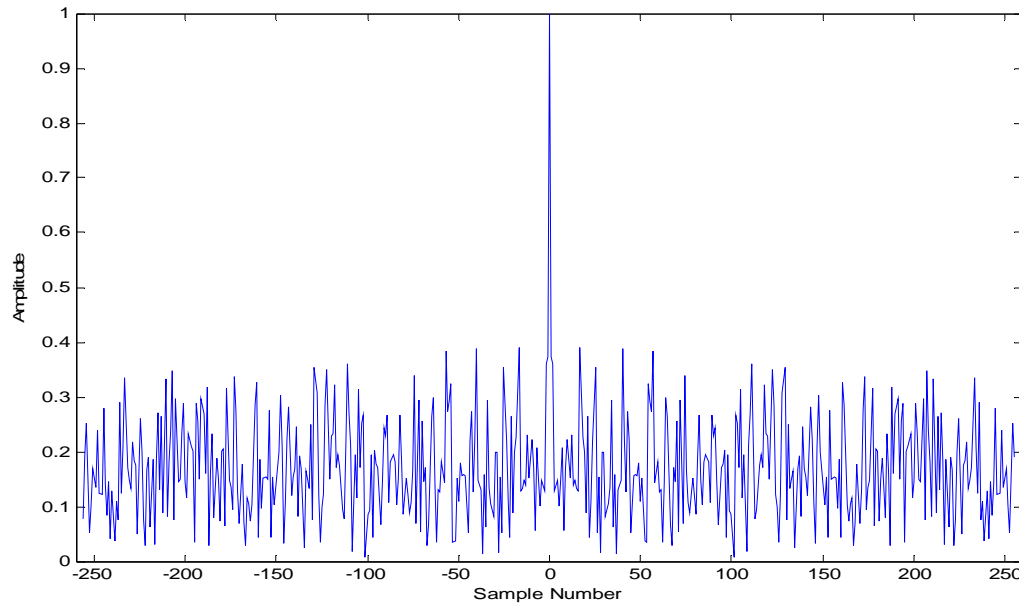


Figure 9.1: Magnitude of peak reduction kernel obtained by projecting an impulse on 26 randomly selected tones for length-512 complex baseband OFDM system.

In practice critical sampled PAR reduction does not give a reliable performance measure so oversampled PAR reduction is used to get a satisfactory performance indication. To perform oversampled PAR reduction an oversampled version of the digital signal is used and the peak reduction kernel is also oversampled by the same factor. Oversampling generally requires a length- NL FFT as compare to N FFT in digital case. So oversampling is L times more computational expensive as compared to digital case and the cost of computing the peak reduction kernel, updating the time domain signal, and peak testing are directly proportional to L . Therefore, the use of oversampling by a factor of L makes the PAR reduction task L times more computational expensive. In our simulations we are using oversampling in time domain, i.e. we are oversampling the signal after the *IFFT* operation. Same is true for the oversampling of peak reduction kernel.

One important issue to consider about oversampling is that it introduces correlation. The samples around a large peak should also be large, and the samples around a small peak should be small. The same is true for the oversampled version of the peak reduction kernel. Therefore an interpolation technique is applied to perform oversampling.

9.1 PAR Reduction Gain with Active-Set Algorithm

In this section we will discuss the PAR reduction performance of active-set algorithm. The performance of active-set algorithm for a target PAR of 7 dB is tested for the complex baseband OFDM symbol of length 2048 and 1024, where 5% of total available tones are used for the generation of PAR reduction signal. The complex baseband signal was approximated by an octagonal boundary. An oversampling factor of $L = 4$ is applied to approximate analog PAR. Up to four active-set iterations are performed on the time domain block. If the PAR of a block is below 7 dB no processing is done on this block. Figures 9.2 and 9.3 show the block PAR CCDF curves for the output time domain OFDM symbols of length 2048 and 1024, respectively. The sample PAR CCDF curves are plotted in the Figures 9.4 and 9.5 for the symbol lengths 2048 and 1024, respectively. For a 10^{-4} block clipping probability, the symbol PAR reduction gains for OFDM symbols of length 2048 after the first four iterations are 1.43, 1.89, 2.23, and 2.54 dB, respectively. Similarly the PAR reduction gains for symbols of length 1024 at the same probability are 1.40, 2.05, 2.35, and 2.77 dB, respectively.

If we look at sample PAR reduction gains after the first four active-set iterations for OFDM symbol of length 2048 we see gains of 0.62, 0.81, 0.96, and 1.09 dB, respectively. These gains are measured at the clipping probability of 10^{-4} .

For the different OFDM symbol lengths, we see that the achievable symbol PAR gain after four iterations is over 2.5 dB. This is a good achievement. The most significant advantage of this approach is that it converges to a suboptimal solution in few iterations with low complexity.

The 16-agonal approximation is implemented using the same parameters described above but in this case OFDM symbols of length 512 and 1024 are simulated. The resulting block PAR CCDF curves are shown in Figures 9.6 and 9.7. In the case of OFDM symbol length of 1024 and 4 active-set iterations a PAR reduction gain of 2.6 dB is achieved at the clipping probability of 10^{-4} .

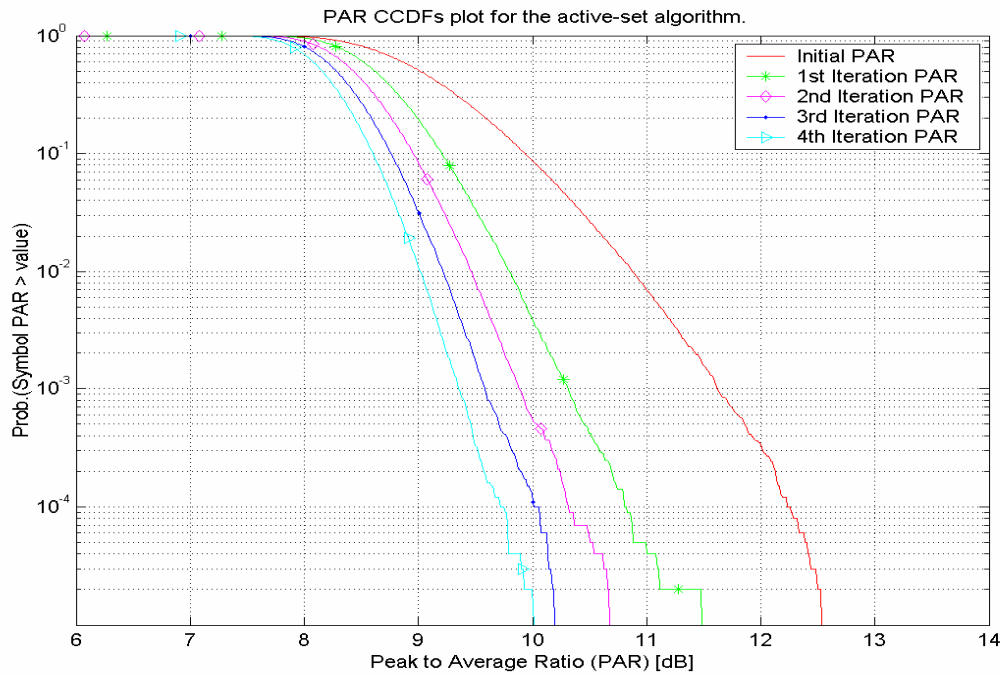


Figure 9.2: Block PAR CCDFs for up to four active-set iterations applied to an OFDM symbols of length 2048, where 5% of total available tones are reserved and an oversampling factor of $L = 4$ is applied.

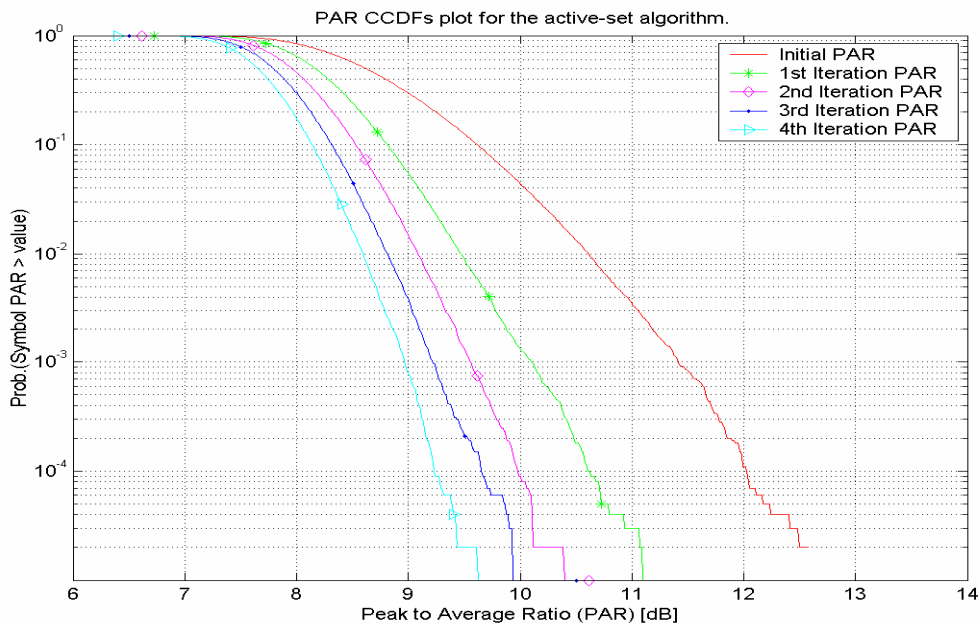


Figure 9.3: Block PAR CCDFs for up to four active-set iterations applied to an OFDM symbols of length 1024, where 5% of total available tones are reserved and an oversampling factor of $L = 4$ is applied.

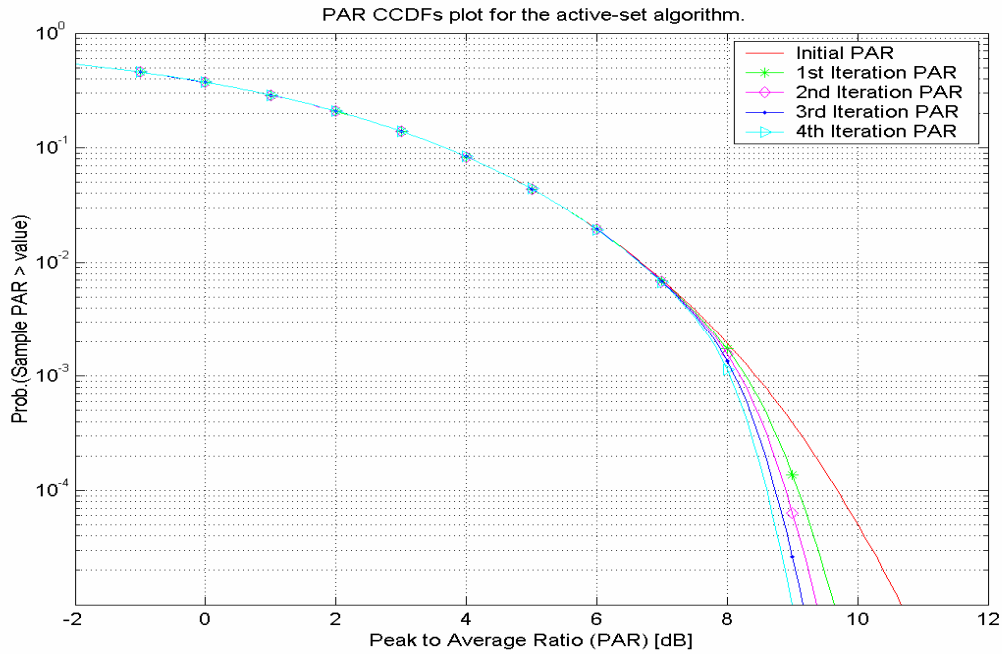


Figure 9.4: Sample PAR CCDFs for up to four active-set iterations applied to an OFDM symbols of length 2048, where 5% of total available tones are reserved and an oversampling factor of $L = 4$ is applied.

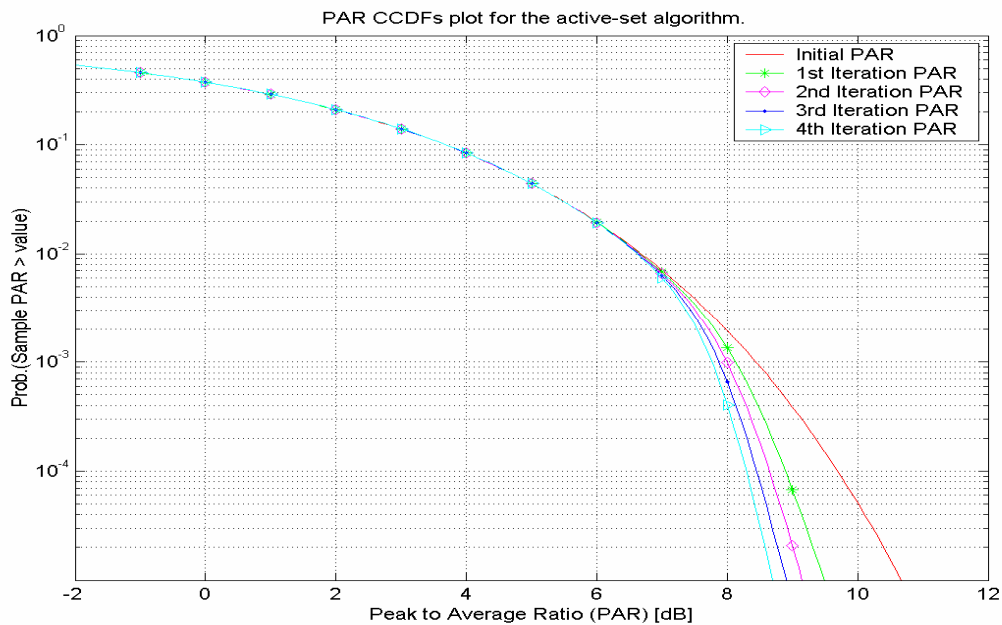


Figure 9.5: Sample PAR CCDFs for up to four active-set iterations applied on an OFDM symbols of length 1024, where 5% of total available tones are reserved and an oversampling factor of $L = 4$ is applied.

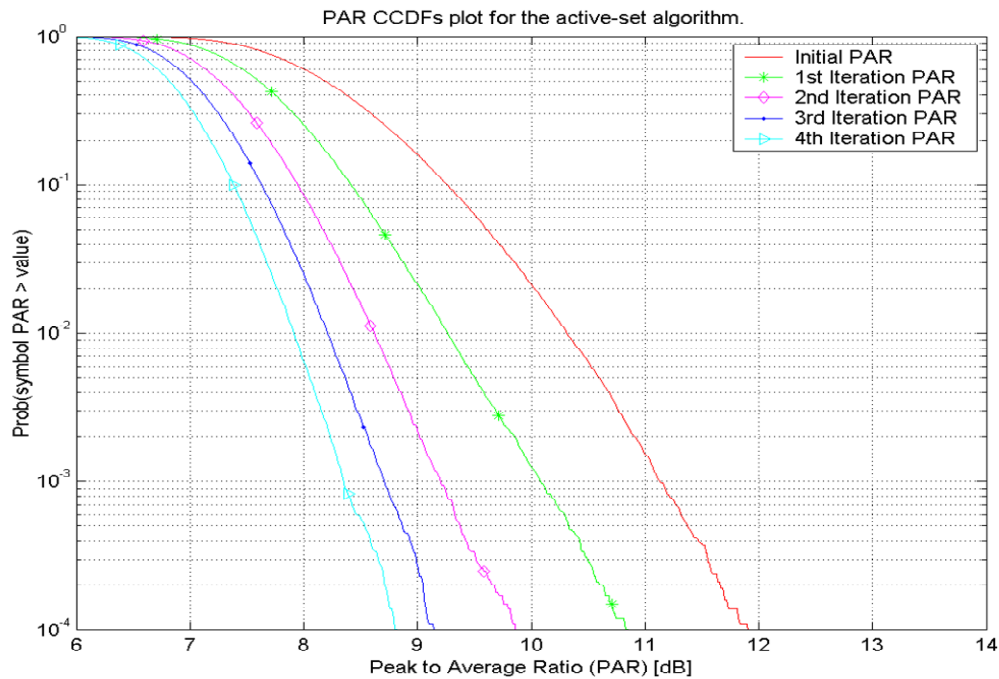


Figure 9.6: Block PAR CCDFs for up to four active-set iterations using 16-agonal approximation applied to an OFDM symbols of length 512, where 5% of total available tones are reserved and an oversampling factor of $L = 4$ is applied.

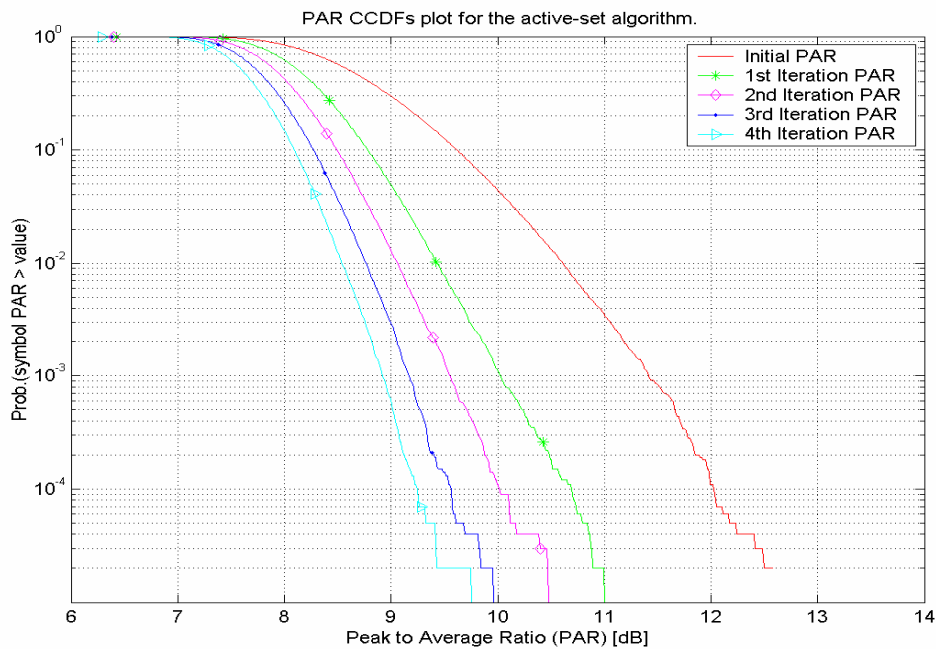


Figure 9.7: Block PAR CCDFs for up to four active-set iterations using 16-agonal approximation applied to an OFDM symbols of length 1024, whereas 5% of total available tones are reserved and an oversampling factor of $L = 4$ is applied.

9.2 Performance Comparison Between Octagonal and 16-agonal Approximation

Octagonal and 16-agonal approximations can be used to approximate the complex baseband OFDM signal. A performance comparison between octagonal and 16-agonal approximation will be discussed here. Octagonal and 16-agonal approximations are simulated for complex baseband OFDM symbols of length 512 and 1024, respectively. An oversampling of $L = 4$ is applied before processing to approximate analog PAR reduction.

Figures 9.8 and 9.9 show the PAR CCDF curves for the first four iterations of the active set algorithm. There are very small PAR reduction differences at various probabilities for the two cases. Results are very similar for different iterations of active-set algorithm. These similarities are due to the slow convergence of the 16-agonal approximation.

As described in Section 3.1.3 the goal in the complex approximation problem is to minimize the peak magnitude of real and imaginary parts of the complex signal sample for all phase rotations. The active set method minimizes the maximum distance to boundary edges. It does not minimize the maximum distance to the corner points where the worst case distances occur. When a signal sample has equal real and imaginary parts then it lies on the corner of the approximating boundary. There are only very few such points on the boundary. In fact one corner point indicates two samples in the active set because the magnitudes of the real and imaginary parts of a sample are considered as two separate optimization points. Assume a sample is on the boundary and very close to a corner. Then there is a high probability that the next iteration of the active set approach will cause this sample to lie on the corner of the new and reduced boundary. The PAR reduction of this iteration will be small. This corner effect has an impact on the convergence speed of the active-set approach. As the size of the polygon boundary increases for better approximation of the circle, the number of corner points increases and the distance between them decreases. This causes the slow convergence towards the optimal solution. So looking at the results in Figures 9.8 and 9.9 we can say that the performance of octagonal approximation is very close to the 16-agonal approximation due to its faster convergence.

From our simulation results we can draw the conclusion that the performance difference between 16-agonal and octagonal is small. The extra computations associated with the 16-agonal approximation are probably not worth implementing in practical systems.

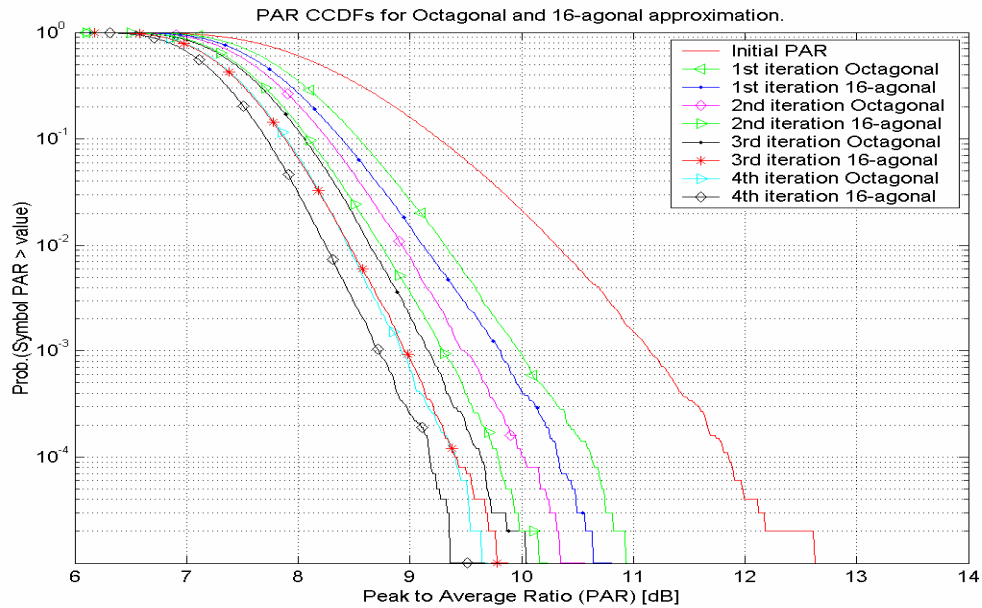


Figure 9.8: Block PAR CCDFs for OFDM symbols of length 512, applying active set PAR reduction with octagonal and 16-agonal approximation. Oversampling by a factor of 4 is applied and 5% of total available tones are reserved.

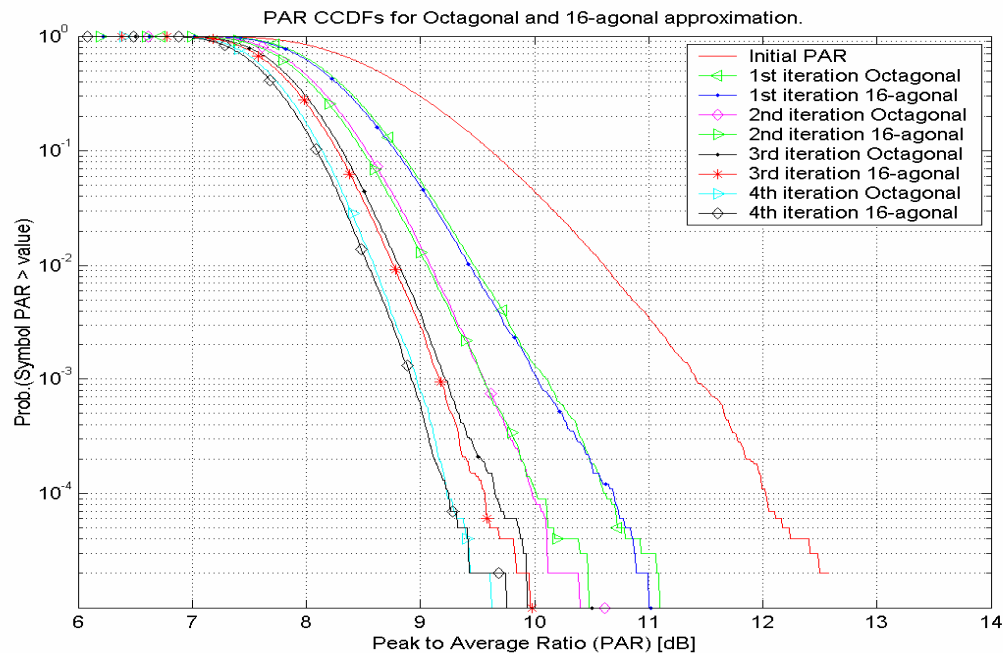


Figure 9.9: Block PAR CCDFs for OFDM symbols of length 1024, applying active set PAR reduction with Octagonal and 16-agonal approximation. Oversampling by a factor of 4 is applied and 5% of total available tones are reserved.

9.3 Investigation of Number of Iterations Required to Achieve a Desired PAR Reduction

The total complexity of the active-set algorithm depends upon the number of iterations and the gain of PAR reduction increases with more iterations. In this section effect of increasing the number of iterations of active-set algorithm on the achieved PAR reduction gain will be analysed and later a statistic about the number of iterations required to achieve a desired PAR will be presented.

Simulations are performed for OFDM symbols of length 1024 and 512, where 5% of total available tones are used for the PAR reduction. First up to five active-set iterations are performed and later the number of iterations is doubled. The final PAR CCDFs after 5 and 10 iterations of active-set algorithm are shown in Figures 9.10 and 9.11, respectively. The target PAR in these cases is 7 dB.

Results show that when number of iterations increases, the PAR reduction gain increases but the difference between the PAR gain after 5 and 10 iterations is not significantly high. The difference in PAR after 5 and 10 iterations is only 1-0.5 dB at various probabilities. Since active-set approach is an interior point method most of the PAR reduction gain is achieved with the first few iterations, i.e. when few peaks (constraints) are active. Very small gains are achieved with the remaining iterations. The complexity of the algorithm depends on the number of iterations. Therefore, a trade-off exists between PAR reduction performance and complexity.

From the simulation results we will draw the conclusion that the active-set algorithm gives most of its PAR reduction gains after the first few iterations. Using up to four iterations yields acceptable PAR levels in most practical cases.

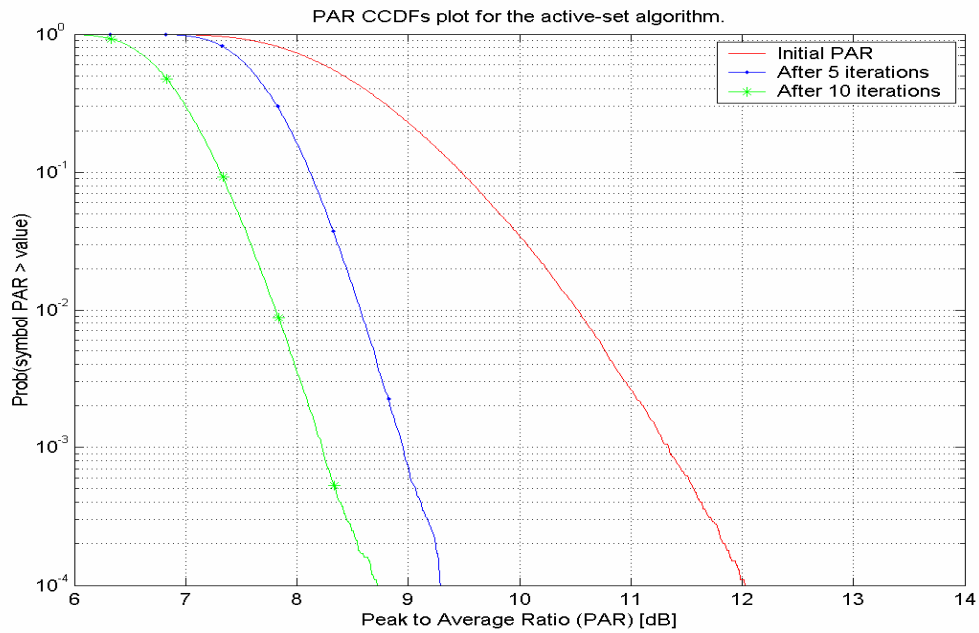


Figure 9.10: Block PAR CCDFs for OFDM symbols of length 1024 when 5 and 10 iterations of the active-set algorithm are applied. Oversampling by a factor of 4 is applied and 5% of total available tones are reserved with target PAR of 7 dB.

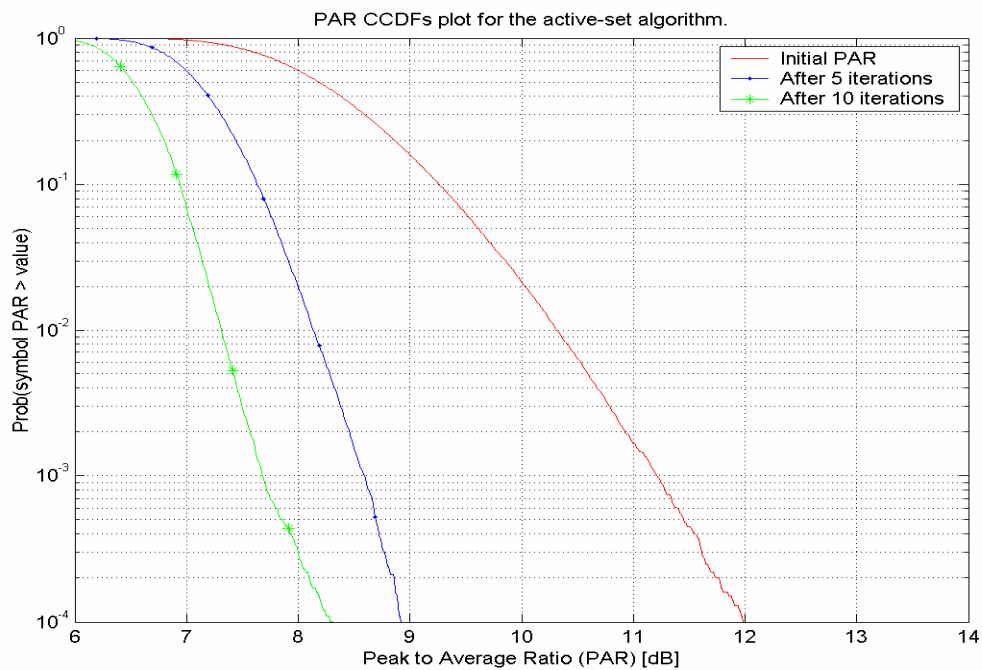


Figure 9.11: Block PAR CCDFs for OFDM symbols of length 512 when 5 and 10 iterations of the active-set algorithm are applied. Oversampling by a factor of 4 is applied and 5% of total available tones are reserved with target PAR of 7 dB.

Figure 9.12 shows the number of iterations to achieve a target PAR of 6, 6.5, and 7 dB with a certain probability. This statistic provides an indication about the number of iteration required to achieve a desired PAR. For example for OFDM symbols of length 512 there is probability of 40% that with five iterations we can achieve a target PAR of 7dB. This result can easily be verified from the PAR CCDF presented previously.

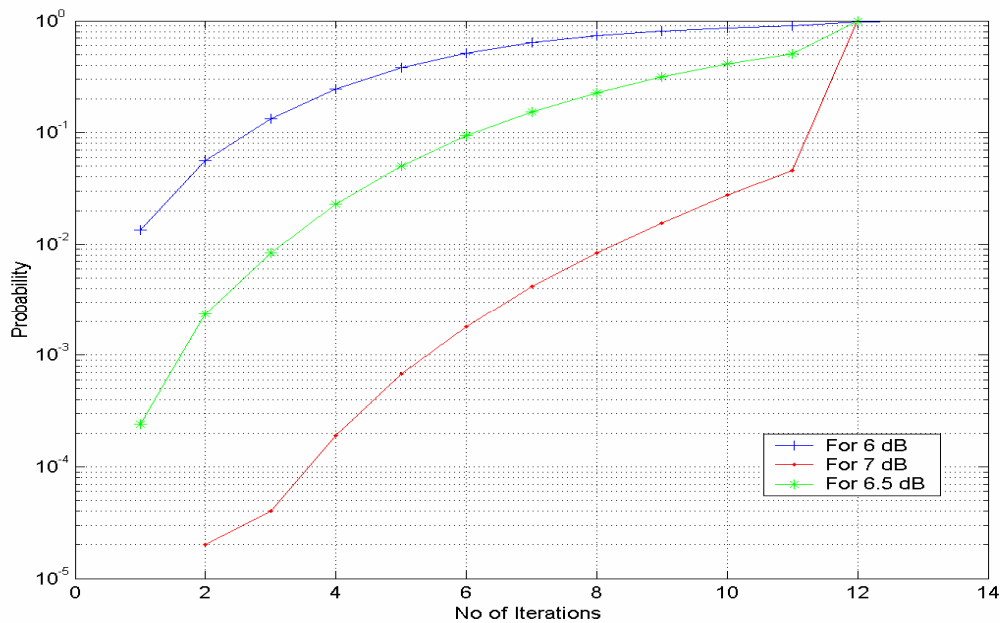


Figure 9.12: Number of iterations CDF for target PAR values of 6, 6.5, and 7 dB when the OFDM symbol length is 512.

9.4 Investigation of Error Power on the Data Tones after Active-Set Method

When PAR reduction is applied on an OFDM symbol and its PAR level still exceeds the target PAR after reduction this OFDM symbol suffers clipping. In frequency domain clipping energy spreads across all tones. Simulations are performed to investigate the error power on data tones after active-set method. The simulated system consists of equal power 16-QAM constellations on 301 out of 512 subcarriers. 26 randomly selected tones (5% of total tones, i.e. 512) are used to generate the PAR reduction signal. Up to four active set iterations are performed with a target PAR of 6, 6.5, and 7 dB.

Figures 9.13, 9.14, and 9.15 show the PSD of the error power on all tones of the OFDM block for a target PAR of 6, 6.5 and 7 dB, respectively.

The average error power on the data tones depends on the target PAR and the resulting percentage of OFDM blocks that require PAR reduction. Results show that the error power on the data tones increases as the target PAR decreases. When the target PAR is low (as in case of 6 dB) many symbols require PAR reduction and have even after reduction a PAR level higher than the set goal. Results show that the average error power on tones varies from -22 to -38 dB which cannot be ignored in the practical systems because it will impact performance.

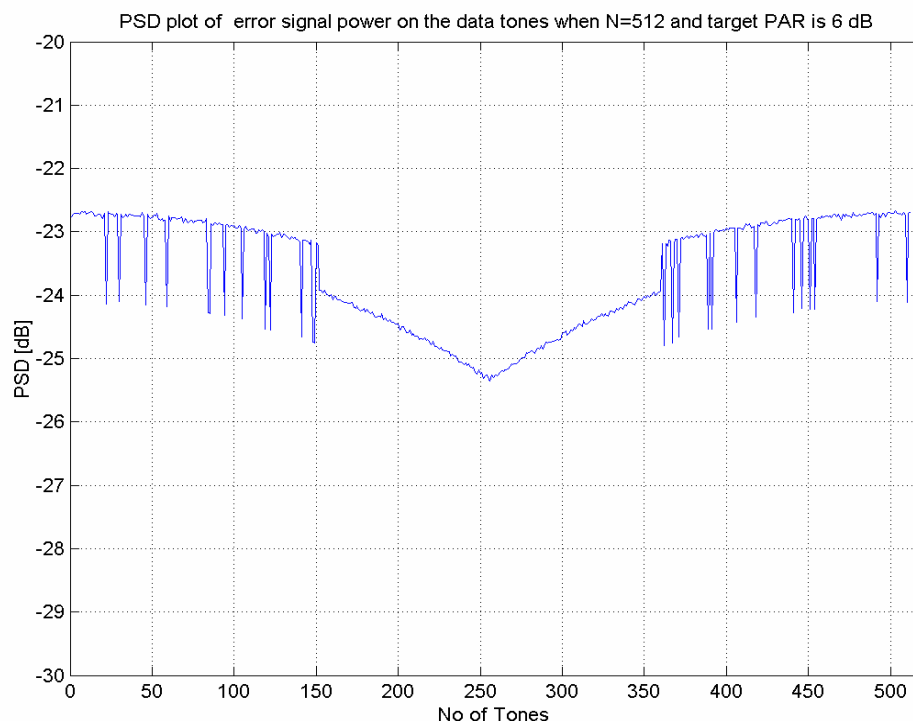


Figure 9.13: PSD of error signal on the data tones after 4 active-set iterations for a target PAR of 6 dB.

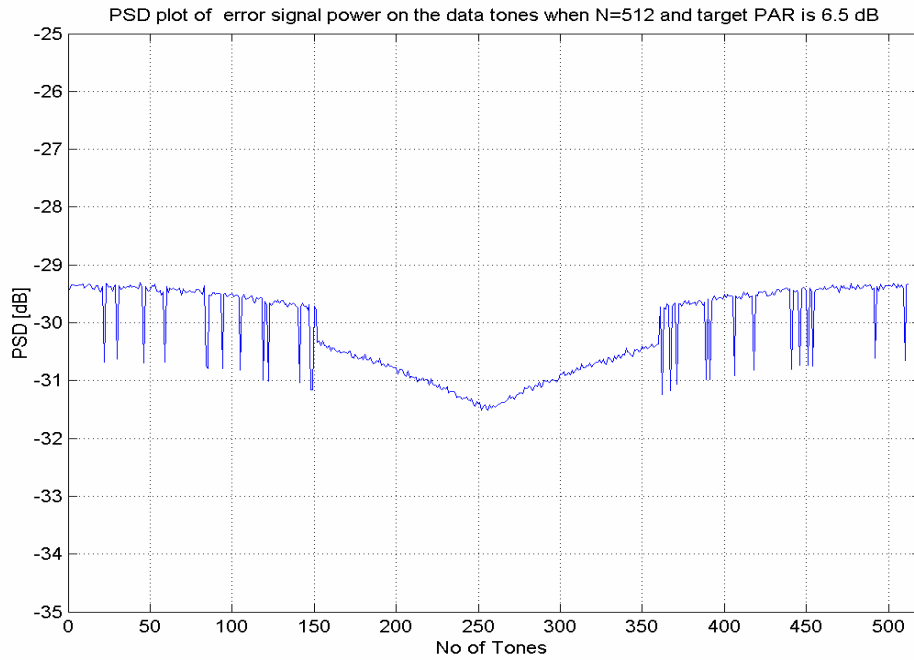


Figure 9.14: PSD of error signal on the data tones after 4 active-set iterations for a target PAR of 6.5 dB.

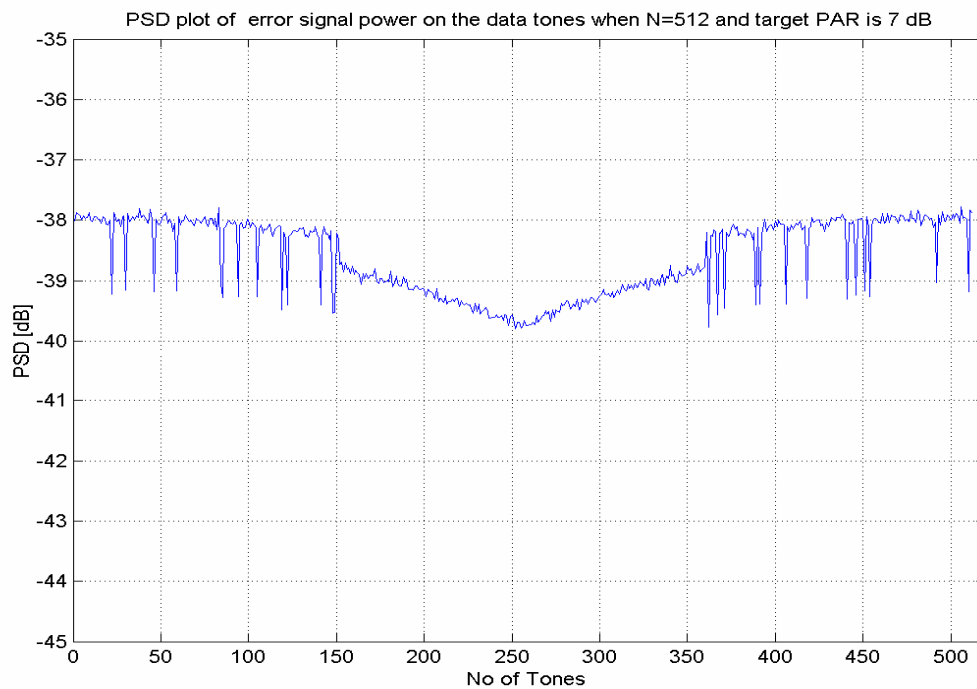


Figure 9.15: PSD of error signal on the data tones after 4 active-set iterations for a target PAR of 7 dB.

9.5 Analysis of PSD Constraints on the Reserved Tones

As described in the Section 7 and 8 a PSD constraint on the reserved tones affect the achievable reduction performance and makes the optimization problem more difficult to solve. To analyse the performance of the active-set algorithm under PSD constraints a low complexity solution is adapted, i.e. to stop at the point where the first reserved tone meets/exceeds the PSD constraint and then quit without using all tones maximally. When any tone reaches its PSD constraint then many or all of the remaining tones in the reserved tone set are not far from reaching there PSD constraints. This low complexity solution is less computationally expensive and result in only a small performance loss from the optimal solution presented in Section 8.

Figure 9.16 shows simulations with the randomly selected 26 tones used for PAR reduction of OFDM symbols of length 512. Oversampling by a factor of 4 is performed before reduction to approximate the analog PAR. The reserved tones have a PSD constraint equal to the data tones. The same simulations are also run for OFDM symbols of length 1024 and 52 reserved tones. Resulting PAR CCDF are shown in Figure 9.17.

As can be seen, the performance of the active-set approach is significantly degraded by this PSD constraint. We are not able to get a PAR reduction gain of more than 0.5 dB. A slight increase in number of reserved tones or iterations does not give a better performance. The PSD limitation on the reserved tones has a significant impact on PAR reduction performance.

Now the simulations are performed using the same parameters as above but the reserved tones are subjected to a PSD constraint of +3, +5 and +10dB relative to the average power of the data tones.

Results show that as the peak power allowed on the reduction tones increases, the performance of the active-set method improves. As discussed in Section 7 the PSD constraints on the reduction tones limits the magnitude of the peak reduction signal to A_{max} . The peak level in an OFDM symbol can be at best reduced to $\max|\mathbf{x}(n)| - A_{max}$.

Loosening the PSD constraint increases A_{max} and we can reduce the maximum magnitude further.

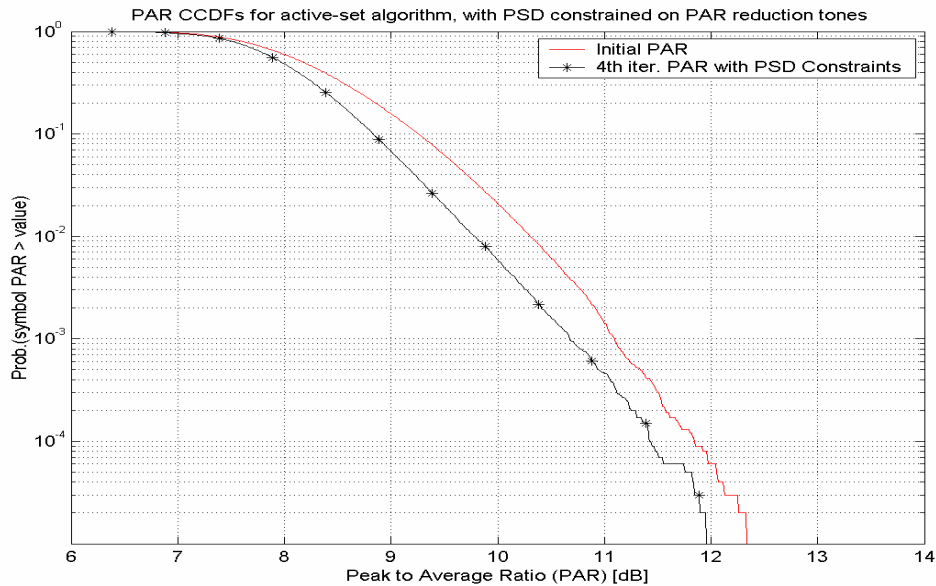


Figure 9.16: Block PAR CCDF for four active-set iterations for OFDM symbols of length 512. The PAR reduction tones must fulfill the same PSD constraint as the data tones. Oversampling by a factor of 4 is applied and 5% of total available tones are reserved with target PAR of 7 dB.

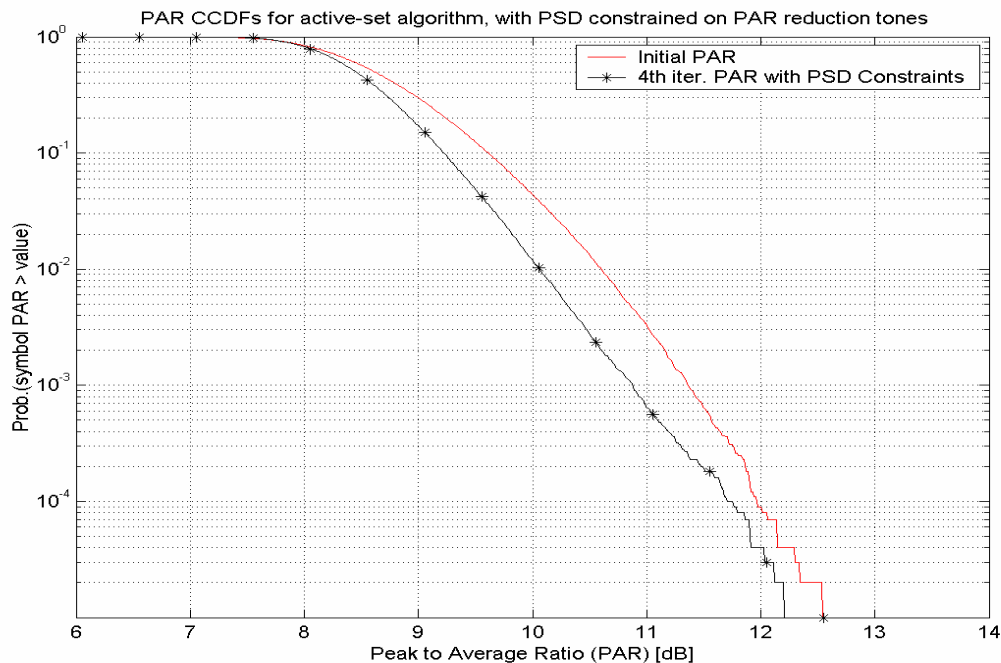


Figure 9.17 Block PAR CCDF for four active-set iterations for OFDM symbols of length 1024. The PAR reduction tones must fulfill the same PSD constraint as the data tones. Oversampling by a factor of 4 is applied and 5% of total available tones are reserved with target PAR of 7 dB.

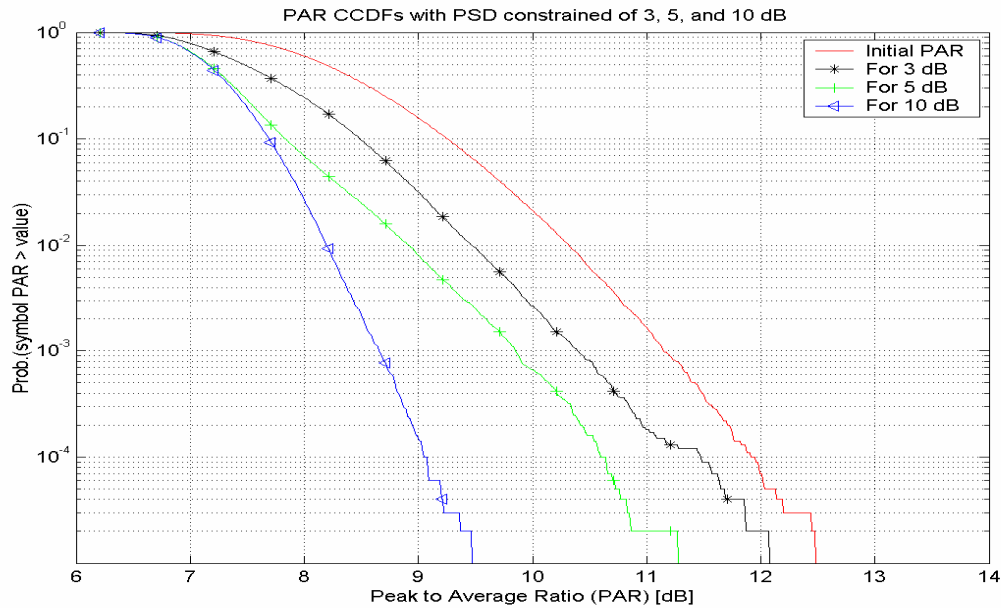


Figure 9.18: Block PAR CCDF for four active-set iterations for OFDM symbols of length is 512. The PAR reduction tones are subjected to a PSD constraint of +3, +5, and +10 dB relative to the average power of the data tones. Oversampling by a factor of 4 is applied and 5% of total available tones are reserved with target PAR of 7 dB.

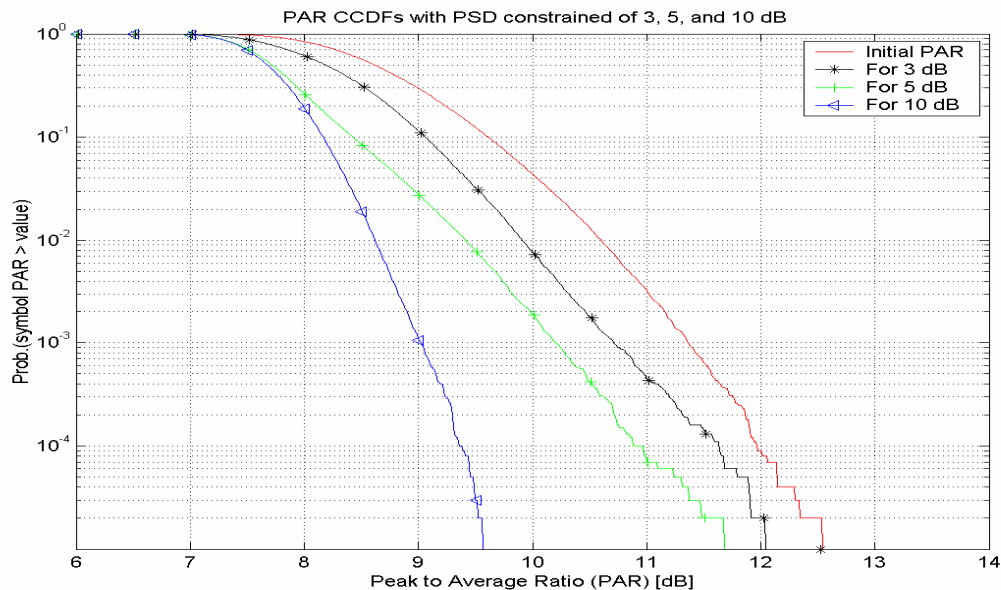


Figure 9.19: Block PAR CCDF for four active-set iterations for OFDM symbols of length is 1024. The PAR reduction tones are subjected to a PSD constraint of +3, +5, and +10 dB relative to the average power of the data tones. Oversampling by a factor of 4 is applied and 5% of total available tones are reserved with target PAR of 7 dB.

9.6 Effect of Number of Reserved Tones

The number of reserved tone is an important factor in the performance of the tone reservation method. Randomly selected tones give a better PAR reduction performance than block placement or equally spaced tones [1]. Using tones for PAR reduction reduces data rate. Therefore a compromise between data rate loss and achieved PAR reduction gain exists. Simulations are performed with OFDM symbols of length 256 and 1024, where 3, 5 and 10 percent of the total available tones are reserved for PAR reduction. Up to four active set iterations are performed. The impact of different numbers of reserved tones on PAR is observed. Figures 9.20 and 9.21 show final PAR CCDF curves for these three cases.

There is no significant difference between the PAR reduction gain when using 3, 5, and 10 percent of total number of tones for PAR reduction.

The performance of tone reservation depends on how well the peak reduction kernel is formed. This is dictated by both the number of reserved tones and also tone placement.

Selecting R tones out of N available tones requires $\binom{N}{R}$ possible combinations. For a system with $N = 256$ and 13 reserved tones (5 % of 256 tones) 10^{21} combinations exist to place these 13 tones. In our simulations we are selecting an optimal tone set total 10000 combinations. The number of combinations increases with increase in the reserved tones. It is obviously impossible to evaluate all different tone placements. This might be a reason that we do not observe any significant difference for the different numbers of reserved tones. But it is the fundamental concept of the tone reservation method that the PAR reduction will increase with increase in number of tones.

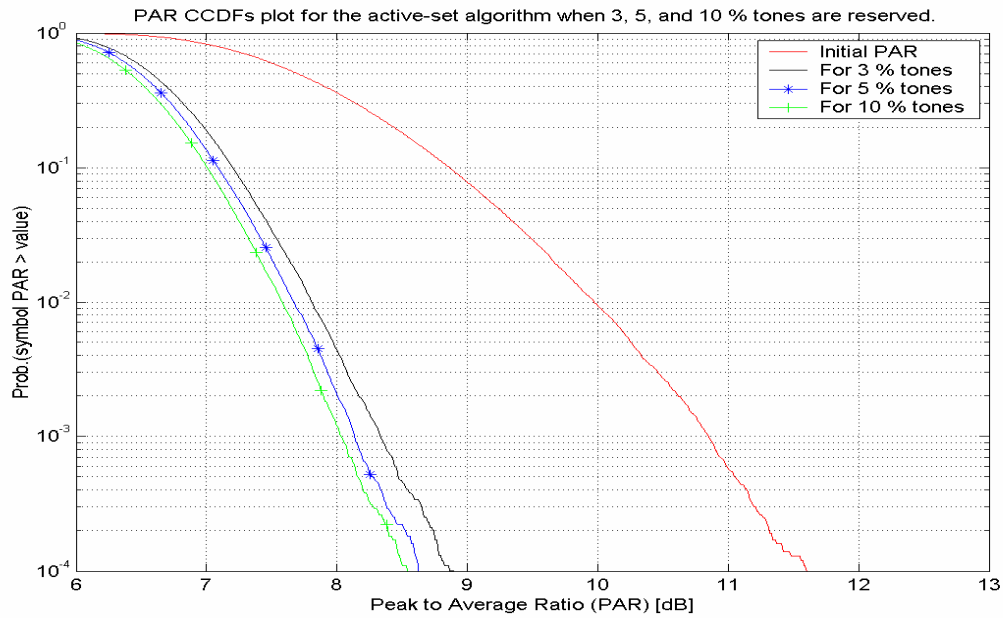


Figure 9.19: Block PAR CCDFs for active-set algorithm when 3, 5, and 10 percent of total tones are reserved for PAR reduction. The OFDM symbol length is 256 and oversampling by a factor of 4 is applied.

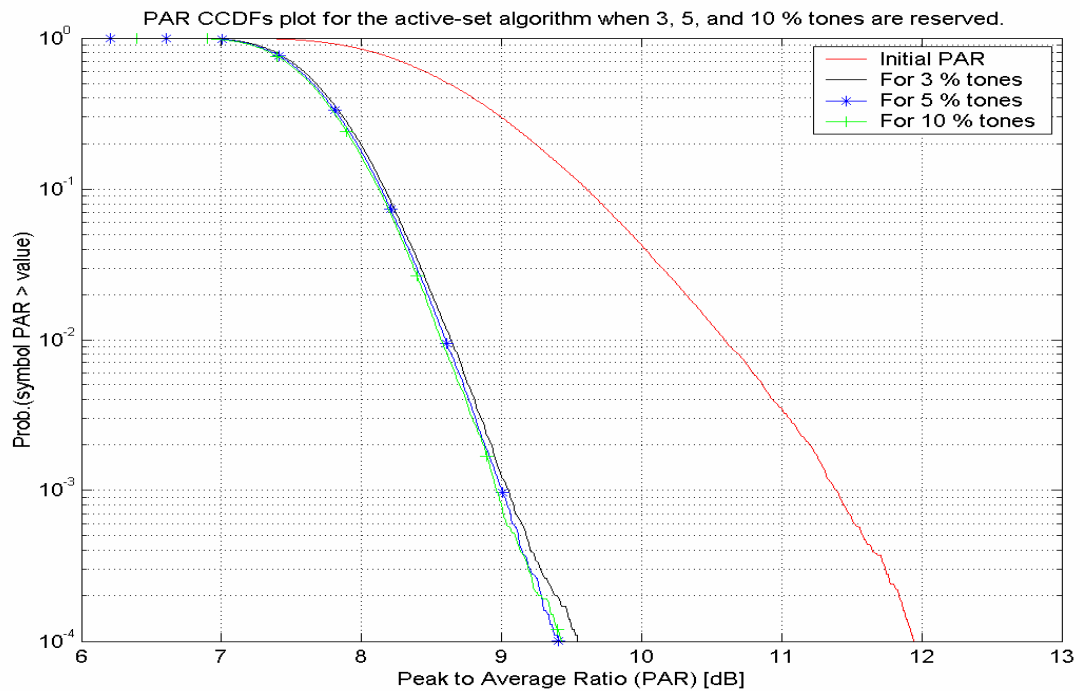


Figure 9.20: Block PAR CCDFs for active-set algorithm when 3, 5, and 10 percent of total tones are reserved for PAR reduction. The OFDM symbol length is 1024 and oversampling by a factor of 4 is applied.

10 Conclusions

The tone reservation method is a valuable technique to reduce the PAR problem. Active set method enhances the tone reservation method performance close to an optimal solution. The main task of this thesis work is to evaluate the active-set performance for complex baseband OFDM signals with and without PSD constraints on the reserved tones.

It has been observed that active set method can give a 3-dB analog block PAR reduction within the first few iterations and with only 3% of the total tones being reserved. Simulations show that the octagonal boundary approximation is more suitable for practical systems.

The performance of the active set method is limited by how well the peak reduction kernel is formed. Both the number of reserved tones but also the location of the reserved tones are key factors in the design and performance of peak reduction kernel. But our simulations do not conform that the PAR reduction gain increases with increase in number of tones.

The average error power on the data tones due to clipping depends on the target PAR and percentage of the OFDM blocks requiring PAR reduction. The average error power impact can not be ignored in practical system designs.

The PSD constraint on the reserved tones degrades the performance of the active set algorithm. When the PSD constraint is very strict then even an increase in the number of reserved tones and number of iterations cannot give a better performance. Relaxing this PSD constraint results in improved PAR reduction gains.

11 Future work

Some possible extensions to this thesis work are

- The least squares approximation of the impulse with equal weight on reduction tones is used to generate the peak reduction kernel. The performance of active-set algorithm can be tested with other forms of peak reduction kernel design such as minimizing the side lobes.
- The performance of the active-set approach suffers from PSD constraint on the reduction tones. The optimal solution of scaling back the step size where the first tone meets PSD constraint can be implemented to analyse the performance improvement.
- The complexity of the algorithm is not considered in this thesis work. The complexity and complexity reduction techniques can be investigated to implement active-set algorithm in real time mobile cellular systems.

12 References

- [1] N. Petersson, "Peak and power reduction in multicarrier systems", Licentiate thesis, Lund University, Lund, Sweden, November 2002.
- [2] B. S. Krongold, "New techniques for multicarrier communication systems", Ph.D. dissertation, University of Illinois at Urbana-Champaign, Urbana, Ill, USA, November 2001.
- [3] A.E. Jones, T.A Wilkinson, and S.K. Barton, "Block coding scheme for reduction of peak to mean envelope power ratio of multicarrier transmission schemes", *Electronics Letters*, Vol.30, No. 25, pp. 2098-2099, Dec.1994
- [4] R. O'Neill and L. N. Lopes, "Envelope Variations and Spectral Splatter in Clipped Multicarrier Signals," in *Proc. PMRC'95*, pp. 71-75, Sept 1995.
- [5] X. Li. and L. J. Cimini, "Effects of Clipping and Filtering on the Performance of OFDM," *IEEE Communications Letters*, Vol. 2, No. 5, pp 131-133, May 1998.
- [6] S.H. Muller, and J.B. Huber, "OFDM with Reduced Peak to Average Power Ratio by Optimum Combination of Partial Transmit Sequences". *IEE Electronics Letters*, Vol. 33, No. 5, pp 368-369 February, 1997.
- [7] A.D.S. Jayalath and C. Tellambura, "Adaptive PTS approach for reduction of peak-to-average power ratio of OFDM signal," *Electronics Letters*, Vol. 36, No. 14, pp. 1226-1228, 2000.
- [8] L. J.Cimini, Jr. and N. R. Sollenberger, "Peak-to- Average power ratio reduction of an OFDM signal using Partial Transmit Sequence with Embedded side information," *IEEE Global Telecommunications Conference*, Vol. 2, pp.746-750, 2000.
- [9] R.W Baml, R.F.H. Fischer, and J.B. Huber, "Reducing the Peak to Average Power Ratio of Multicarrier Modulation by Selected Mapping". *IEE Electronics Letters*, Vol. 32, No. 22, pp 2056-2057 September 1997.
- [10] E.Lawrey, C. J.Kikkert, "Peak to Average Power Ratio reduction of OFDM signals using Peak Reduction Carriers".
- [11] J. Tellado-Mourello, "Peak to average power reduction for multicarrier modulation", Ph.D. dissertation, Stanford University, Stanford, Calif, USA, September 1999.
- [12] D. L. Jones, "Peak power reduction in OFDM and DMT via active channel modification", in *Proc. Asilomar Conference on Signals, Systems, and Computers*, vol. 2, pp. 1076-1079, Oct. 1999.

- [13] A. Gatherer and M. Polley, "Controlling clipping probability in DMT transmission," in Proc. Asilomar Conference on Signals, Systems, and Computers, vol. 1, pp. 578–584, Pacific Grove, Calif, USA, November 1997.
- [14] D. G. Luenberger, "Linear and Nonlinear Programming", Addison-Wesley, Boston, Mass, USA, 1984.
- [15] P. Ödling, N. Petersson, A. Johansson, and P. O. Börjesson, "Howmuch PAR to bring to the party?" in Proc. Nordic Signal Processing Symposium, Tromsø– Trondheim, Norway, October 2002.
- [16] N. Petersson, A. Johansson, P. Ödling, and P. O. Börjesson, "Analysis of tone selection for PAR reduction," in Proc. International Conference on Information, Communications and Signal Processing, Singapore, October 2001.
- [17] X. Chen and T. Parks, "Design of FIR filters in the complex domain," IEEE Trans. Acoustics., Speech, Signal Processing, vol. ASSP-34, pp. 144–153, Feb. 1987.
- [18] N. Petersson, A. Johansson, P. Ödling, B. S.Krongold and P. O. Börjesson, "PSD-constrained PAR Reduction for DMT/OFDM" EURASIP journal on Applied Signal Processing 2004:10, pp.1498-1507.
- [19] Brian S Krongold and Douglas L. Jounes, "An Active-Set Approach for OFDM PAR Reduction via Tone Reservation" IEEE Transactions on Signal processing. VOL. 52, No 2, February 2004.